

Interactive comment on “Aerosol particle formation in the upper residual layer” by Janne Lampilahti et al.

Janne Lampilahti et al.

janne.lampilahti@helsinki.fi

Received and published: 10 December 2020

We thank the Referee for the comments. Please see our answers below.

Comment: A number of previous studies, i.e., Nilsson et al. (2001), Stratmann et al. (2003), Stanier et al. (2004); (Wehner et al., 2007), and (Platis et al., 2016) suggested that enhanced turbulent mixing, related to the growth of daytime convective boundary layer and the lift of the inversion could cause downward mixing of the particles, which had already grown in size. In addition, there have been several recent studies that point out direct evidence for NPF occurring aloft, in the interface between the shallow convection and inversion (Chen et al., 2018; Größ et al., 2018). By using turbulence statistics and the boundary layer dynamics (Meskhidze et al., 2019) and (Zimmerman

Printer-friendly version

Discussion paper



et al., 2020) quantified the frequency of the residual layer and the ground level nucleation events and assessed their contributions (relative to other sources) to the near-surface fine particle number budgets during different seasons. The authors don't seem to acknowledge many of these studies. That leaves the impression that the residual layer nucleation and the particle entrainment into the mixed layer is a novel mechanism for explaining the appearance of >10 nm-sized particles at the near-surface layer. I would encourage the authors to clearly discuss how their research builds upon these prior studies and highlight the similarities.

Answer: In order to put this study into context we added the following background to the Introduction:

"NPF has been observed in various environments and at various altitudes inside the troposphere. The majority of NPF observations come from ground-based measurements (Kerminen et al., 2018; Kulmala et al., 2004), which can be argued to represent NPF within the mixed layer (ML). Measurements from aircrafts show that NPF is also common in the upper free troposphere (FT) (e.g. Clarke and Kapustin, 2002; Takegawa et al., 2014). Entrainment of particles formed in the upper FT was identified as an important source of CCN in the tropical boundary layer (BL) (Wang et al., 2016; Williamson et al., 2019). Measurements from high-altitude research stations also demonstrate that NPF frequently takes place in the FT, in these cases NPF was often observed in BL air that was transported to the higher altitudes (Bianchi et al., 2016; Boulon et al., 2011; Rose et al., 2017; Venzac et al., 2008).

When studying the vertical distribution of NPF in the lower troposphere one has to consider the evolution and dynamics of the BL. Nilsson et al. (2001) found that the onset of turbulent mixing correlated better with the onset of NPF at ground level than with the increase in solar radiation. The authors gave several hypotheses to why this might be. One hypothesis was that NPF starts aloft, either in the RL or in the inversion capping the shallow morning ML. As the turbulent mixing starts, the newly formed particles would be transported down and observed at the ground-level.

C2

ACPD

Interactive
comment

Printer-friendly version

Discussion paper



Many observations have supported the hypothesis put forward by Nilsson et al. (2001). Größ et al. (2018), Meskhidze et al. (2019) and Stanier et al. (2004) reported positive correlation between the onset of NPF at ground level and the breakup of the morning inversion due to beginning of convective mixing. Chen et al. (2018), Platis et al. (2015) and Siebert et al. (2004) used in situ airborne measurements and observed that NPF started during the morning on the top of a shallow ML capped by a temperature inversion at a few hundred meters above ground. The particles grew to detectable nucleation mode (sub-25 nm) sizes aloft, and when the ML began to grow due to thermally-driven convection, the particles were mixed downwards and observed at the ground-level where they further continued to grow in size. Stratmann et al. (2003) observed newly formed particles inside the RL disconnected from the shallow ML or the inversion that capped it. Furthermore, Wehner et al. (2010) observed that NPF inside the RL was connected to turbulent layers. On the other hand, Junkermann and Hacker (2018) attributed their observations of elevated ultrafine particle layers at few hundred meter altitudes in the RL to flue gas emissions from stacks with subsequent chemistry taking place during air mass transport over long distances.

The hypothesis proposed by Nilsson et al. (2001) was based on observations done in Hyytiälä, Finland, which is a rural site surrounded by boreal forests and with very clean air. However, the supporting evidence comes from measurements done in more polluted environments in Central Europe and USA. Airborne measurements done over Hyytiälä have not found NPF on top of the shallow morning ML or within the bulk of the RL, instead the NPF events seem to start within the ML (Boy et al., 2004; Laakso et al., 2007; O'Dowd et al., 2009). This might be because in the more polluted environments the RL and/or the shallow ML contains high enough concentrations of precursor vapors from anthropogenic sources, so that NPF can be initiated in the morning inversion and/or within the bulk of the RL. Interestingly, though, observations from Hyytiälä using a small instrumented airplane have frequently found nucleation mode particle layers above the ML at a much higher altitude range of ~1500-2800 m above ground and the explanation for these layers is not clear (Leino et al., 2019; Schobesberger et al.,

2013; Väänänen et al., 2016). For example Väänänen et al. (2016) found that for the 2013-2014 airborne measurement campaigns 16/36 (~44%) profiles showed a sub-25 nm particle layer above the ML at altitudes greater than 1800 m asl.

In this study we used co-located airborne and ground-based measurements to study nanoparticles over a boreal forest in Hyytiälä, Finland. We aimed to characterize the elevated nucleation mode particle layers that were a frequent observation in the previous studies. Specifically we were looking at the following questions: (1) where in terms of atmospheric layers, how often and why do these aerosol particle layers occur, and (2) how they are related to ground-based observations, and what implications this has for data interpretation."

Comment: The airplane flight profiles seem to be different between Fig. 3 and Fig. 4. Are these two different profiles? If so, please explain.

Answer: There was a mistake in the time range given in the Fig. 3 caption. The correct time range is 12:00-13:12. Furthermore we combined the May 2, 2017 case study figures into a single figure (Fig. 1).

Comment: Fig. 4 shows that the negative flux was measured at the surface starting at 9:30 am. However, according to Fig. 3, there was no significant vertical gradient between the surface and the 1000 m. Please explain the presence of strongly negative fluxes between 9:30 am and 12:30 pm. According to Fig. 4, a new 10 nm particle mode only appeared at the ground-level at 12:35 pm. So, what causes negative fluxes in the morning?

Answer: The previous correction to the time range should remove the confusion here. In addition we added some text about the particle mode and the negative flux in the morning:

"At the ground level a new particle mode with lower number concentration coupled with negative particle flux also appeared at around 10:00. It may be that these particles

ACPD

Interactive
comment

Printer-friendly version

Discussion paper



were also mixed down from higher altitudes, but in the absence of airplane measurements during that time, we cannot be sure."

Comment: Please include several more case studies so the reader can compare the similarities and contrast the differences. For each case study please show the normalized spectral density plots so the reader can ascertain that there was indeed a growth event following the appearance of >10 nm-sized particles at the near-surface layer.

Answer: While a particle layer was observed on multiple flights, it is rare to find cases where one can directly observe a particle layer mixing down from the airplane and link the ground-based observations to the airborne observations. Ideally the BL development should also be clear in the lidar and the soundings so that comparison can be made to the aerosol observations. We added one more case study (May 19, 2018) to the paper. The case is analyzed in the below text and Fig. 2:

"3.2 Case study: May 19, 2018

On May 19, 2018 another case of nucleation mode particles mixing down into the ML was observed. Figure 4A shows that during the airplane's ascend the lower edge of the particle layer was observed at ~ 1200 m asl and the top of the layer was at 2000 m asl. The N3-10 increased in the layer from ~ 1000 cm⁻³ up to ~ 10000 cm⁻³. When the airplane descended back into the ML the N3-10 was increased to around 6000 cm⁻³ throughout the ML, suggesting that the particle layer was mixed into the ML. The air masses arrived from a similar sector as in the May 2, 2017 case. SO₂ and CO concentrations in Hyytiälä remained low when the particles were mixed down (0.05 ppb and 127 ppb for SO₂ and CO, respectively).

Figure 4B shows particle number size distribution measurements from the measurement airplane and from the field station. The particle layer was observed as increased number concentration in the smallest size channels of the SMPS at 9:00 before the airplane flew above the ML. Roughly 20 minutes later a similar-sized particle mode appeared in the ground-based data. For this day there were no particle flux data. The

C5

ACPD

Interactive
comment

Printer-friendly version

Discussion paper



new particle mode continued to grow larger inside the ML for several hours.

Figure 4C shows the TKE dissipation rate on May 18-19, 2018 from Hyytiälä and temperature soundings from Jokioinen. On May 18, 2018 the ML went up to 2500 m asl in Hyytiälä. The Jokioinen soundings show that at 6:00 the top of the RL was at about 1800 m asl, marked by the subsiding inversion left from the previous day's ML. The particle layer mixed down from approximately 2000 m asl."

Comment: Please include the flux values for each of the 8 cases shown in Fig. 8. Since the DMPS was running at the ground site, it would be interesting to know the detected start and the end time of the events, as well as the growth rate for different size particles.

Answer: We added a table that summarizes the cases and includes the negative particle flux peak values (picture of the table in Fig. 3). Regarding the growth rates we added the following sentence to the text:

"The mean growth rate of the appearing particle modes was 2.2 nm h⁻¹ which is similar to 2.5 nm h⁻¹ reported by Nieminen et al. (2014) for 3-25 nm particles during NPF events in Hyytiälä."

Comment: Fig. 8 shows 6-hour differences between the times when the mixed layer reaches the top of the residual layer. Please provide an explanation based on the full analysis of the meteorological data.

Answer: We added the following paragraph to the end of section 3.5 in order to explain these differences:

"The time that the ML reaches the upper RL depends on the height of the RL, which in turn depends on the height of the ML on the previous day and the rate at which the top of the RL subsides. The mixing time also depends on the rate at which the ML on the day of interest grows. For example on March 28, 2014 the ML height on the previous day and the RL height during the night were 1300 m and 1100 m, respectively. On

ACPD

Interactive
comment

Printer-friendly version

Discussion paper



April 4, 2014 the corresponding numbers were 2800 m and 2200 m. Because of this on March 28, 2014 the ML reached the upper RL much earlier at ~7:00 compared to April 4, 2014 when the ML reached the upper RL at ~11:00. For example on April 15, 2014 the ML grew slowly in the morning due to presence of low clouds that limited thermal convection. Because of this the ML reached the top of the RL relatively late at 13:00"

Comment: Please compare the monthly fractions of new particle formation events (Fig. 9) in Hyytiälä with the data reported in other studies discussed above.

Answer: We added the following paragraphs comparing the studies:

"The monthly distribution of upper RL NPF events follows the distribution of ML NPF events, with a peak during spring (Mar-May). This is in line with previous studies that classified NPF events in Hyytiälä (Dal Maso et al., 2005; Nieminen et al., 2014). This makes sense since the conditions favoring ML NPF would also favor upper RL NPF. However, Buenrostro Mazon et al. (2009) and Dada et al (2018) found that the tail events and transported events had a peak during the summer months (Jun-Aug).

On 16% of the NPF event days NPF only took place in the upper RL but not in the ML. This number is smaller than the 36% found by Dada et al. (2018) for transported events and the 26% found by Buenrostro Mazon et al. (2009) for tail events. This might be because we restricted to cases where a negative peak in particle flux was associated with the appearance of nucleation mode particles. For example, a case where the particles were horizontally advected to the measurement site would not be expected to cause a negative peak in the particle flux and therefore would not be classified as upper RL NPF."

References not cited in earlier versions:

Boulon, J., Sellegri, K., Hervo, M., Picard, D., Pichon, J.-M., Fréville, P. and Laj, P.: Investigation of nucleation events vertical extent: a long term study at two

[Printer-friendly version](#)[Discussion paper](#)

different altitude sites, *Atmospheric Chemistry and Physics*, 11(12), 5625–5639, doi:<https://doi.org/10.5194/acp-11-5625-2011>, 2011.

Venzac, H., Sellegri, K., Laj, P., Villani, P., Bonasoni, P., Marinoni, A., Cristofanelli, P., Calzolari, F., Fuzzi, S., Decesari, S., Facchini, M.-C., Vuillermoz, E. and Verza, G. P.: High frequency new particle formation in the Himalayas, *PNAS*, 105(41), 15666–15671, doi:[10.1073/pnas.0801355105](https://doi.org/10.1073/pnas.0801355105), 2008.

O'Dowd, C. D., Yoon, Y. J., Junkermann, W., Aalto, P., Kulmala, M., Lihavainen, H. and Viisanen, Y.: Airborne measurements of nucleation mode particles II: boreal forest nucleation events, *Atmospheric Chem. Phys.*, 9(3), 937–944, doi:[10.5194/acp-9-937-2009](https://doi.org/10.5194/acp-9-937-2009), 2009.

Boy, M., Petäjä, T., Dal Maso, M., Rannik, Ü., Rinne, J., Aalto, P., Laaksonen, A., Vaatovaara, P., Joutsensaari, J., Hoffmann, T., Warnke, J., Apostolaki, M., Stephanou, E. G., Tsapakis, M., Kouvarakis, A., Pio, C., Carvalho, A., Römpp, A., Moortgat, G., Spirig, C., Guenther, A., Greenberg, J., Ciccioli, P. and Kulmala, M.: Overview of the field measurement campaign in Hyytiälä, August 2001 in the framework of the EU project OSOA, *Atmospheric Chem. Phys.*, 4(3), 657–678, doi:[10.5194/acp-4-657-2004](https://doi.org/10.5194/acp-4-657-2004), 2004.

Laakso, L., Grönholm, T., Kulmala, L., Haapanala, S., Hirsikko, A., Lovejoy, E. R., Kazil, J., Kurten, T., Boy, M., Nilsson, E. D., Sogachev, A., Riipinen, I., Stratmann, F. and Kulmala, M.: Hot-air balloon as a platform for boundary layer profile measurements during particle formation, *Boreal Environ. Res.*, 12(3), 279–294, 2007.

Nieminen, T., ssmi, A., Dal Maso, M., Aalto, P. P., Keronen, P., Petäjä, T., Kulmala, M. and Kerminen, V.-M.: Trends in atmospheric new-particle formation: 16 years of observations in a boreal-forest environment, *Boreal Environ. Res.*, 19, 191–214, 2014.

Interactive comment on *Atmos. Chem. Phys. Discuss.*, <https://doi.org/10.5194/acp-2020-923>, 2020.

ACPD

Interactive
comment

Printer-friendly version

Discussion paper



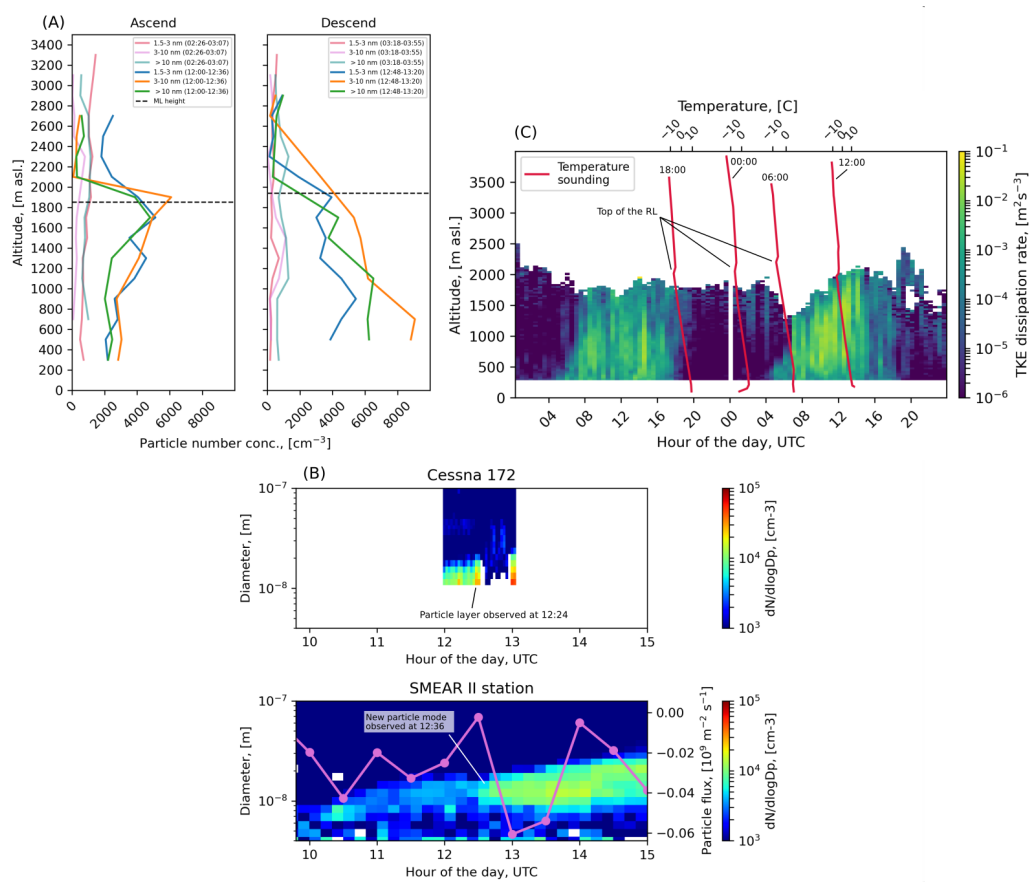


Fig. 1.

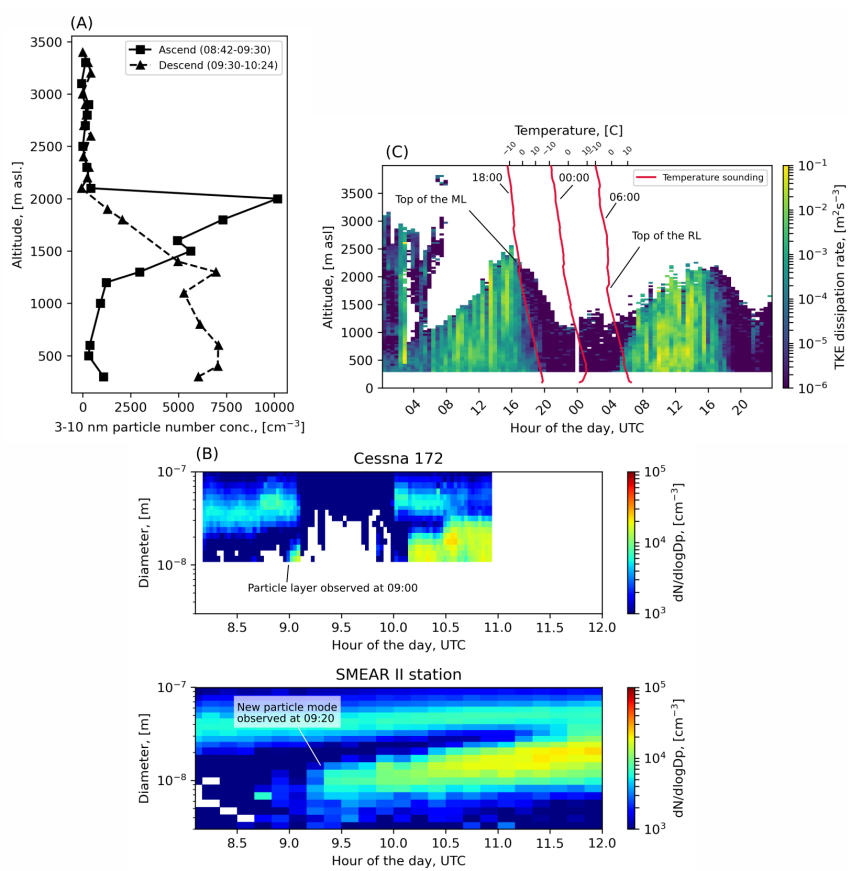


Fig. 2.

Table 1: rl_h = residual layer height during night or early morning (m asl), rl_ht = time when the rl_h was observed (time when the sounding was released, hour of the day, UTC), mode_t = nucleation mode particle mode first appears (hour of the day, UTC), mode_t1/mode_t2 = nucleation mode particle mode appearance confidence interval (hour of the day, UTC), rl_t = new mixed layer reaches the top of the residual layer (hour of the day, UTC), rl_t1/rl_t2 = new mixed layer reaches the top of the residual layer confidence interval (hour of the day, UTC), bl_h = observed maximum height of the previous day's boundary layer (m asl.), dp = mean mode diameter for the newly appeared particle mode, when they first appear (nm), gr = growth rate calculated for the newly appeared particle mode (nm h^{-1}), pf = the value of the negative particle flux peak ($10^9 \text{ m}^{-2} \text{ s}^{-1}$).

date	rl_ht	rl_h	mode_t1	mode_t	mode_t2	rl_t1	rl_t	rl_t2	dp	bl_h	pf	gr
20140328	5.3	1100	8.5	9	9.5	5.5	7	8	20	1300	-0.25	2.28
20140331	7.6	2400	14	14.5	15	12	13.5	14	10	2200	-0.06	2.1
20140404	8.5	2200	10.5	11	11.5	10.5	11	11.5	8	2800	-0.04	1.39
20140409	5.5	1500	9	9.25	9.5	6	6.5	7	8	1800	-0.13	1.18
20140415	5.3	1600	14.5	14.25	15	12	13	14	11	1700	-0.18	1.94
20140422	0.0	1800	12	12.5	13	10.5	11	11.5	17	1900	-0.17	1.0
20140518	0.0	1500	9.5	10	10.5	8	8.5	9	13	1900	-0.11	2.91
20140705	5.3	1500	11	11.5	12	8.5	9	10	12	1700	-0.1	4.83

Fig. 3.

Printer-friendly version

Discussion paper



Atmos. Chem. Phys. Discuss.,
https://doi.org/10.5194/acp-2020-923-AC2, 2020
© Author(s) 2020. This work is distributed under
the Creative Commons Attribution 4.0 License.

Interactive comment on “Aerosol particle formation in the upper residual layer” by Janne Lampilahti et al.

Janne Lampilahti et al.

janne.lampilahti@helsinki.fi

Received and published: 11 December 2020

We thank the Referee for the comments. It is suggested that the nucleation mode particle layers we observed might have originated from elevated upwind pollution sources, such as power station flue stacks.

As an example air mass back trajectories for the May 2, 2017 case study are shown. It is noted that the air masses arriving at 1800 m altitude above Hyttiälä at 12 UTC (this is where the aerosol particle layer was observed) traveled over a power station few hours prior to arriving in Hyttiälä.

We tested the emission hypothesis by checking if the entrained particle layer was associated with increased SO₂/CO concentrations. We observed no increase in the pollu-

Printer-friendly version

Discussion paper



tant concentrations during the day or when the particles mixed down (Fig. 1). Therefore we believe it is unlikely that these particles originated from the power station emissions.

We also checked the pollutant concentration for the second case study (May 19, 2018) we added to the manuscript (see our answer to Referee #1) and no increase in pollutant concentrations was observed when the particles mixed down at around 9:20 (Fig. 1).

Junkermann and Hacker (2018) explains that the flue stack emissions are usually released to altitudes below 400 m. In Finland the tallest chimneys are well below 200 m agl. The particle layers we observed from the Cessna were on average between 2300-2700 m above Hyytiälä. During daytime when the BL is mixing flue stack emissions would be mixed throughout the mixed layer and then stay in the residual layer the following night. One would not expect a distinct layer at the top of the RL to form. If the emissions were released into the residual layer during night, they would remain at roughly the same altitude due to lack of vertical transport during night and not be transported to the top of the RL. We think that in this case the better explanation is that the nanoparticles were formed aloft.

Comment: What are the ambient conditions relevant to particle formation or aging in the residual layer, temperature, humidity, water vapor concentration, wind speed and direction, potential condensation sink? Are aging nano-particles in this layer growing or shrinking (Kerminen et al, 2018 and references cited therein)?

Answer: According to Alonso-Blanco et al. (2017) conditions in the residual layer that would favor particle shrinkage are lack of sunlight during night and dilution because the air is cleaner. After sunrise the increased solar radiation at higher altitudes would not favor particle shrinkage. Also the lower temperature would not favor particle shrinkage. After sunrise increased solar radiation, low pre-existing aerosol particle surface area and cold temperatures would favor NPF. NPF would probably not be taking place during the night due to lack of solar radiation

Comment: 40 km is a wide range, see Fig. 1. Where is the GPS-location of the

C2

ACPD

Interactive
comment

Printer-friendly version

Discussion paper





measurements with respect to well known locations of major precursor molecule and/or primary nanoparticle emissions upwind? What is the flight pattern during ascents and descents? Can this be used to derive wind data from example from GPS when the Lidar is not sensitive enough?

Answer: The majority of flights were centered over Hyytiälä. We modified Figure 1 in the manuscript to also show the horizontal distribution of measurements (Fig. 2). Notable emission sources close to this area would be the city of Tampere ~ 60 km SW (population ~ 250000) from Hyytiälä and the Korkeakoski sawmill ~ 6 km SE from Hyytiälä (Eerdekens et al., 2009). When we flew over Tampere the effect on particle number concentrations was always clear. Usually the >3 nm number concentrations increased to about 5000 cm^{-3} from the background 2000 cm^{-3} at couple hundred meters above the ground.

Also we noticed the 2011-2018 dataset was not restricted to this 40 km radius from Hyytiälä. So we remade the Figures 1 and 6 in the manuscript with the 40 km boundary condition. The average vertical number-size distribution in Figure 6 did not change much but the 3-10 nm bin showed slightly negative values above the ML. For the updated figure we only used the SMPS data (Fig. 3). Also for the temperature profile we only considered profiles when there was an increased (larger than 75th percentile) sub-25 nm number concentration in the RL (2000-3000 m).

The flight patterns were straight legs perpendicular to the mean wind direction while ascending or descending. So at least the wind direction can be inferred from the direction of the flight legs.

Comment: Why are the measurements in the ascend beginning at 200 m, the descend ends at 600 m agl? Teisko, ~ 15 km (alt 158 m) from Hyytiälä (alt 178 m) would be a location for missed approaches and legal low altitude flying. O'Dowd et al (2009) presented profiles nearly to the ground from QUEST 2003.

Answer: We extended the lowest altitude bin to 200-400 m asl (Fig. 4). The descend

ended at 500 m asl during that flight.

Comment: Are there any indicators for example from the Hyytiälä meteorological tower that can be related to vertical mixing intensity? Potential parameters could be surface temperature or temperatures in the vertical profile. Glider pilots use ground based temperature measurements for a decision when to take off.

Answer: There is a 3d anemometer close to canopy, so in principle turbulence intensity above the canopy could be calculated.

Comment: Although an SMPS is onboard there is no size distribution presented for the case study. A complete size distribution would be a mandatory information for the interpretation as it carries information about the age of the particles (and potential distance to the source location).

Answer: We added the size distribution (Fig. 4)

Comment: For comparison of airborne and ground based data the same parameters, particle size distributions and not particles on the aircraft and air ions on the ground, should be used.

Answer: We added the particle size distribution from SMEAR II (Fig. 4). The downside is that the time resolution is not as good (10 min instead of 4 min)

Comment: Whether the vertical profiles within 2 1/2 hours in the early afternoon and another flight in the morning are comparable at all remains open, see the HYSPLIT trajectories above. The vertical profiles of the morning flight including air mass history and trajectory need to be included as well.

Answer: We changed the text to say: "During this flight no elevated particle layer was observed and the number concentrations were quite uniform with altitude in the different size ranges, staying below 1500 cm⁻³." The profiles are included in Fig. 4.

Comment: To investigate, whether the 1.5 nm particles grow into the size range of

ACPD

Interactive
comment

Printer-friendly version

Discussion paper



3-20 nm and to disentangle between NPF in a sulphur rich environment and primary emissions a better size resolution is necessary (Junkermann et al, 2011a). See there and in subsequent papers size distributions with a finer resolution in the range below 10 nm. It needs a lagrangian flight pattern to confirm that air mass change is excluded, see Junkermann and Hacker (2015)

Answer: The SMPS measurements onboard (going down to 10 nm) and the ground-based measurements at the SMEAR II station (going down to 4 nm in the Fig. 4, the smallest size channel was noisy) do not show multiple nucleation modes. The gas measurements at the field station do not suggest sulphur rich environment.

One interpretation is that the particles were horizontally advected to the site in another air mass. However the particle layer was observed aloft first and then ~ 15 min later at the field station coupled with a downward peak in particle flux suggesting that the particles were mixed down from aloft.

Comment: The observations in the 3-20 nm range are well in agreement with the patchy structure of particle number and size distributions from previous studies in the area (O'Dowd et al, 2009, Schobesberger et al, 2013, Väänänen, et al, 2016, Leino et al, 2019) as well as the patchwork blanket of power station plumes shown by Junkermann et al (2016). All these studies point towards a significant contribution from local emission hotspots. Chemical analysis from 20 years of particle research at Hyytiälä reveals that sulphur molecules and likely ammonia are among the key substances required for the production of nanoparticle clusters. A recent publication by Hao et al (2018) about measurements at Hyytiälä even requires particulate sulphate in the residual layer mixed downward to explain the observations on the ground.

Answer: In the studies mentioned the patchiness was observed inside the mixed layer but not above. It seems there are few sub-25 nm particles above the mixed layer in Hyytiälä, except for the top of the RL (Fig. 3).

The patchiness of nucleation mode particles can have other explanations such as vari-

[Printer-friendly version](#)[Discussion paper](#)

able cloud cover (Wehner et al., 2007), land features (O'Dowd et al., 2009), and organized convection like roll vortices (Lampilahti et al., 2020).

Comment: The sources of such sulfate particles in the atmosphere are well known and typically linked to burning processes (Bigg and Turvey, 1978, Ayers et al, 1979, Whitby et al, 1978). In Finland these sources are mostly located along the coastline, about 200 km or approximately 5-6 hours upwind of Hyytiälä, (Fig. 1, www.endcoal.org). Further examples for primary nanoparticle size, aging and emission rates are shown in the papers of Junkermann et al.

Transport via the residual layer is not an exclusive pattern, veering plumes from wind direction changes in the planetary boundary layer can explain as well the observations without additional aerosols in the residual layer (examples: O'Dowd et al, 2009, for Hyytiälä under conditions with snow covered ground or Laaksonen et al, 2005 (SPC, Italy) Junkermann and Hacker (2018)). In all cases 3D-meteorology is the key for analysis of these observations.

Answer: We do observe increased aerosol particle concentrations in the top parts of the RL. The case studies (May 2, 2017 and May 19, 2018) and ground-based observations from the BAEEC campaign fit the idea that particles are mixing down from the top of the RL.

With such moving emission plumes we would expect to see changes in SO₂/CO concentrations but for example in the case studies this was not observed.

Comment: Recent and historic literature is not always taken into account. There are not many airborne studies of nanoparticles, but they should be included.

Answer: We extended the Introduction, see the answer to Referee #1.

Comment: Time within the manuscript is mixed between UTC and Eastern European Summer Time (EEST) in figures and text

Answer: All time should be fixed to UTC now.

C6

ACPD

Interactive
comment

Printer-friendly version

Discussion paper



Comment: Fig. 5: Scales for Theta and water vapor are missing. The figure is not really supportive, it suggests a high mixed layer at night although the upper rim of the Lidar data reflect only the vertical range of the measurements. Significant TKE for vertical mixing is restricted only to daylight hours.

Answer: We added temperature soundings on top of the lidar data (Fig. 4). The point of showing the temperature soundings was to show where the temperature inversion was and it agrees with the mixed layer height based on TKE dissipation rate. During the night the vertical mixing reduces but the temperature inversion remains present and shows where the top of the night time residual layer was. In all the figures where we show the lidar data and the soundings we added the temperature scale to the top.

Comment: please take into account: a few hours upwind of Hyytiälä one of Finland's largest pollution source emits 150 kg sulphur dioxide / hour located, emitting both a large amount of primary particles and a mixture of substances relevant to nanoparticle formation independent on the time of the day

Answer: We added the following paragraph to the case study

"The air masses came from the Arctic Ocean over northern Scandinavia. They went over the west coast of Finland where there are known pollution sources (most notably the Vaskiluoto coal-fired power plant), however in Hyytiälä the SO₂ and CO levels remained low all day (~0.025 ppb and ~115 ppb for SO₂ and CO, respectively). Even when the particles were observed at the surface no increase in pollutant concentrations was observed. Pollution released into the night time RL from elevated sources such as flue gas stacks would be expected to form layers at roughly the altitudes where the emissions occurred below few hundred meters. This is because of the lack of vertical mixing. If the pollution was released during daytime into a ML, it would be uniformly mixed into the ML and stay like that in the RL during night (Junkermann and Hacker, 2018). The likely explanation for sub-10 and sub-3 nm particles at this altitude is NPF."

Comment: Fig. 9 should be discussed in terms of the annual variability of meteorology,

[Printer-friendly version](#)[Discussion paper](#)

for example the intensity of convection under typical weather conditions in Finland. The intensity of the vertical mixing process described in the manuscript is dependent on surface conditions (snow until the end of March?) and surface and vertical profile temperatures throughout the year.

Answer: The days were sunny spring days without snow (and one sunny day in July). On such days the ML is expected to be well-mixed and the particles should reach the surface in less than an hour or so (Stull, 1988). We looked at the soundings released at ~11:20 and ~17:20 from Hyytiälä during these days. The approximately constant potential temperature profiles suggest a well-mixed layer (Fig. 5).

Comment: Fig. 10 is outdated and needs severe revision. Sources are not always on the ground they can be elevated as well

Answer: We will add some trees to represent biogenic emissions and smokestacks to represent anthropogenic emissions of precursors. However relative to the ~2.5 km asl altitude where the particle layers were on average observed (Fig. 3) we find it does not make much difference to distinguish between sources that are at ~150m altitude or at surface.

Comment: Platis et al 2015 should be Platis et al, 2016

Answer: 2015 should be correct (see: <https://link.springer.com/article/10.1007/s10546-015-0084-y>)

Comment: Junkermann and Hacker (2018) is cited in the text but missing in the reference list.

Answer: It is added to the list

References:

Alonso-Blanco, E., Gómez-Moreno, F. J., Núñez, L., Pujadas, M., Cusack, M. and Artíñano, B.: Aerosol particle shrinkage event phenomenology in a South Euro-

pean suburban area during 2009–2015, *Atmospheric Environment*, 160, 154–164, doi:10.1016/j.atmosenv.2017.04.013, 2017.

Eerdekens, G., Yassaa, N., Sinha, V., Aalto, P. P., Aufmhoff, H., Arnold, F., Fiedler, V., Kulmala, M. and Williams, J.: VOC measurements within a boreal forest during spring 2005: on the occurrence of elevated monoterpene concentrations during night time intense particle concentration events, *Atmospheric Chemistry and Physics*, 9(21), 8331–8350, doi:https://doi.org/10.5194/acp-9-8331-2009, 2009.

Wehner, B., Siebert, H., Stratmann, F., Tuch, T., Wiedensohler, A., Petäjä, T., Dal Maso, M. and Kulmala, M.: Horizontal homogeneity and vertical extent of new particle formation events, *Tellus B*, 59(3), 362–371, doi:10.1111/j.1600-0889.2007.00260.x, 2007.

O'Dowd, C. D., Yoon, Y. J., Junkermann, W., Aalto, P., Kulmala, M., Lihavainen, H. and Viisanen, Y.: Airborne measurements of nucleation mode particles II: boreal forest nucleation events, *Atmos. Chem. Phys.*, 9(3), 937–944, doi:10.5194/acp-9-937-2009, 2009.

Lampilahti, J., Manninen, H. E., Leino, K., Väänänen, R., Manninen, A., Buenrostro Mazon, S., Nieminen, T., Leskinen, M., Enroth, J., Bister, M., Zilitinkevich, S., Kangasluoma, J., Järvinen, H., Kerminen, V.-M., Petäjä, T. and Kulmala, M.: Roll vortices induce new particle formation bursts in the planetary boundary layer, *Atmospheric Chemistry and Physics*, 20(20), 11841–11854, doi:https://doi.org/10.5194/acp-20-11841-2020, 2020.

Stull, R. B.: *An Introduction to Boundary Layer Meteorology*, Softcover reprint of the original 1st ed. 1988 edition., Springer, Dordrecht., 1988.

Interactive comment on *Atmos. Chem. Phys. Discuss.*, https://doi.org/10.5194/acp-2020-923, 2020.

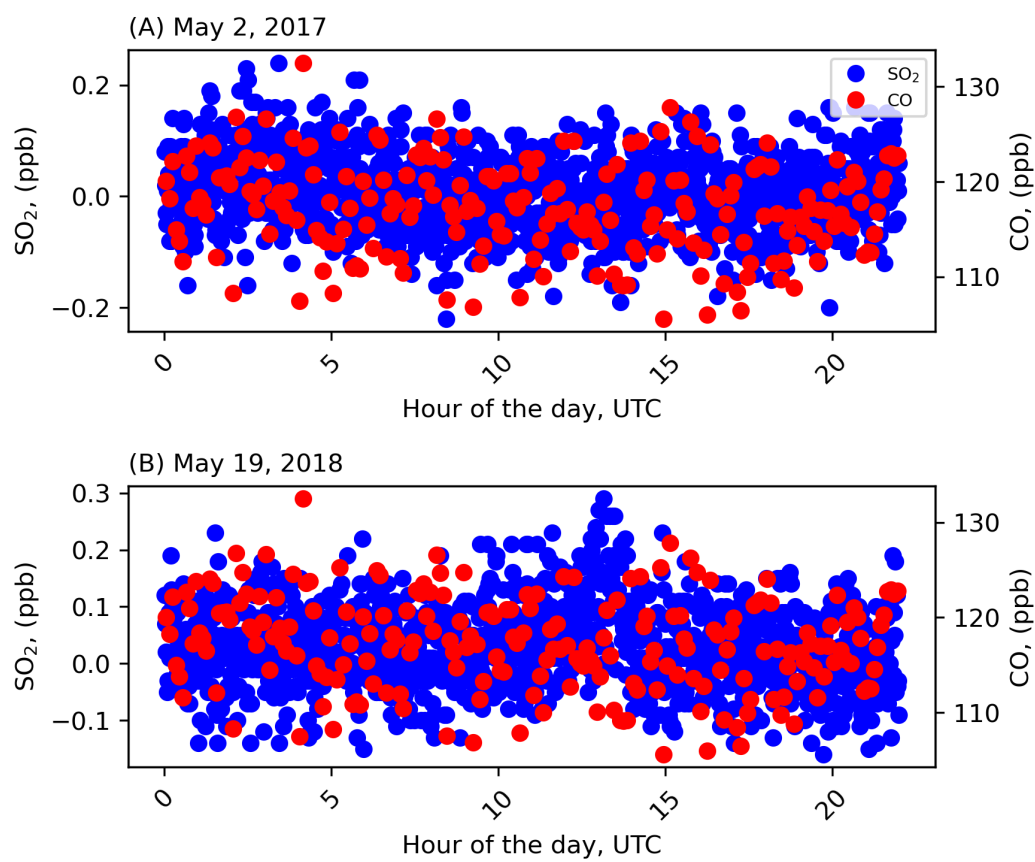
ACPD

Interactive
comment

Printer-friendly version

Discussion paper



**Fig. 1.**

C10

[Printer-friendly version](#)[Discussion paper](#)

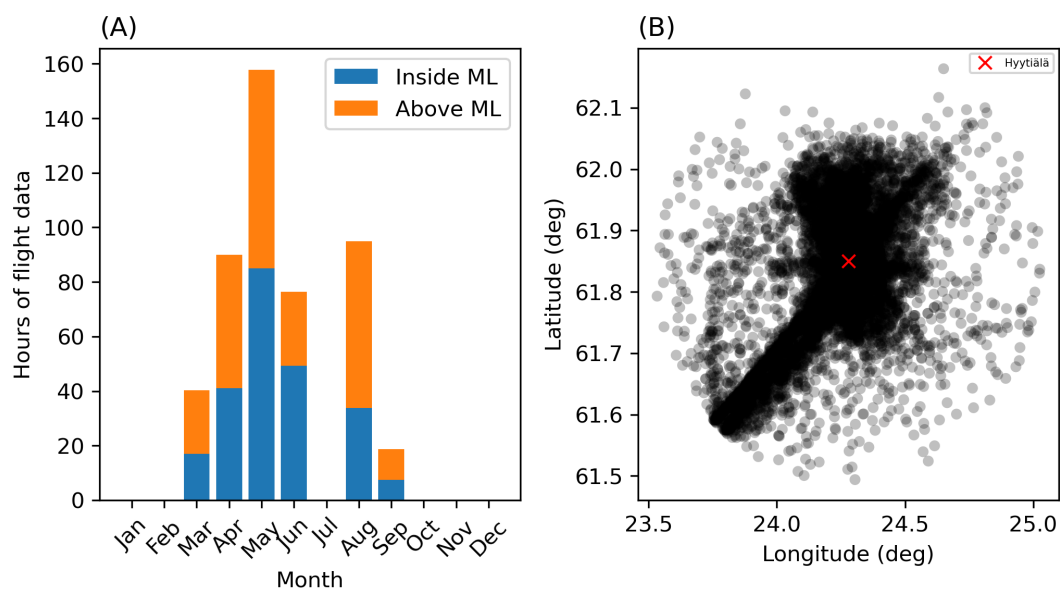


Fig. 2.

[Printer-friendly version](#)[Discussion paper](#)

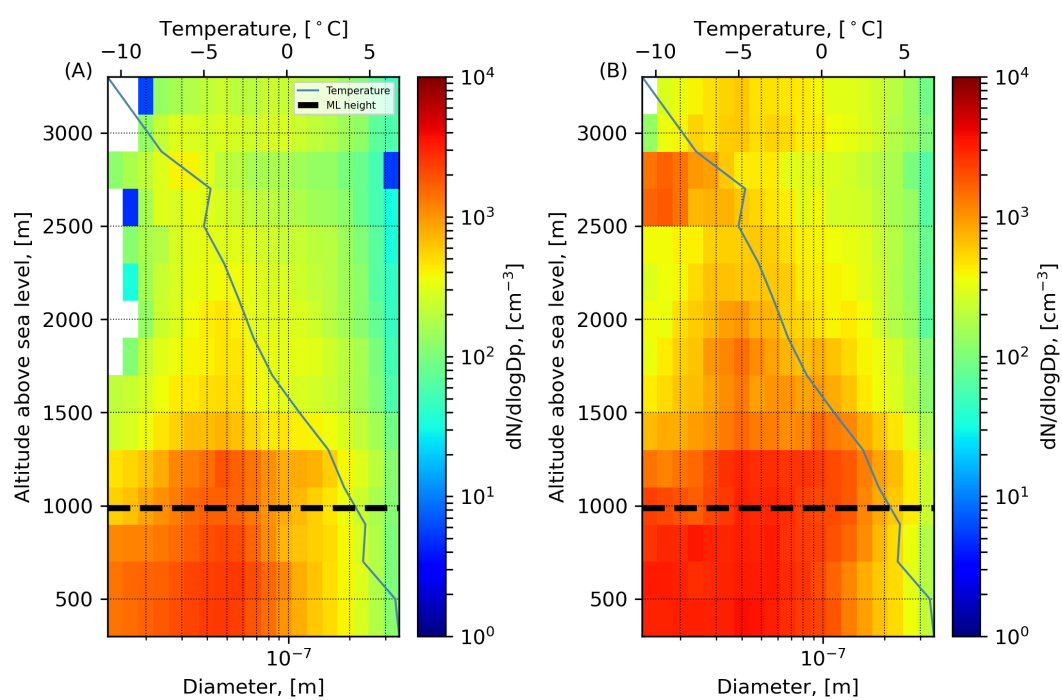


Fig. 3.

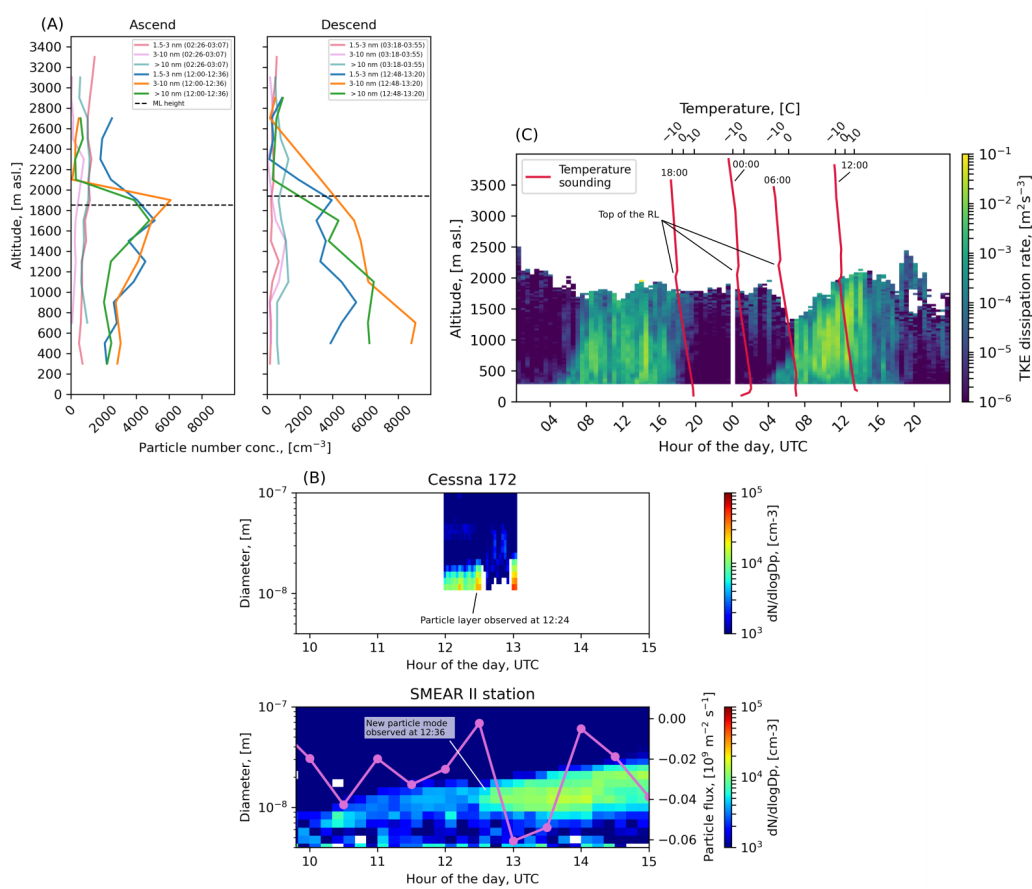


Fig. 4.

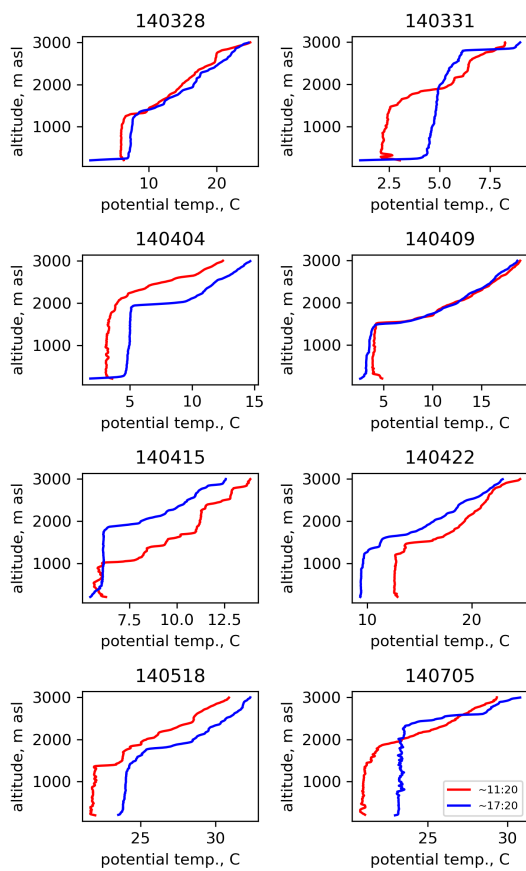


Fig. 5.

Interactive comment on “Aerosol particle formation in the upper residual layer” by Janne Lampilahti et al.

Janne Lampilahti et al.

janne.lampilahti@helsinki.fi

Received and published: 12 December 2020

We thank the Referee for the comments. Our responses are below:

Comment: Roughly isokinetic sampling : Could you please be more precise. The inlet is either isokinetic with a control of the flow within the inlet or not isokinetic. It seems that you are controlling it with a valve and with a constant speed of the Cessna. Therefore most of the time the sampling should be isokinetic. However, roughly is too vague. What are the deviation from the isokinetic conditions ? This condition has a large impact on the measurement quality and therefore on their validity. Please correct and add more information about that.

Answer: From Schobesberger et al (2013) (reference in the manuscript): "The aerosol

Printer-friendly version

Discussion paper



inlet's design was adopted from the University of Hawai'i shrouded solid diffuser inlet design originally presented in McNaughton et al. (2007) for use aboard a DC-8 aircraft. Our inlet is a downsized version of it, suiting the lower cruising speed of the Cessna."

Detailed characterization of the inlet can be found in McNaughton et al. (2007). In our measurement range (<400 nm) the inlet losses should be negligible.

Inside the main sampling line the velocity of sample air was ~ 2 m/s (~ 47 lpm controlled by a manual valve), while the instruments (UCPC: 1.5 lpm, PSM: 2.5 lpm, SMPS: 1 or 4 lpm) drew the air at the core sampling inlets between ~ 0.5 -2 m/s. Under these conditions considerations of isokinetic sampling are not necessary. So we removed this part from the text.

Comment: Figure 3 analysis : "The layer had increased number concentrations of sub-20nm and sub-3nm particles." in comparison to what ? The descent profile ? I think you should clearly name the reference you are comparing these results to. Moreover, you should definitely show the profiles from the early morning flight on Figure 3. That would raise no doubts that the aerosol layer was not present before the sun rise and that could give the reader a clear reference. "at this point there were no signs of the particle layer" This is misleading. The layer didn't disappear spread into lower layers, in this case the ML. Is there a threshold for the RL height ? I believe the highest is the better due to lower temperature and cleaner air. But is there any RL height range for those events ? Could you also add the ML height in this figure ?

Answer: We added the particle number concentrations in the different size ranges at altitudes below/above and in the layer to the text.

We also added the particle number concentration vertical profiles from the early morning ascend/descend to the figure (Fig. 1).

We removed the misleading sentence and instead wrote: "The airplane entered back into the ML at 12:56 and the particle number concentration was increased throughout

ACPD

Interactive
comment

Printer-friendly version

Discussion paper



the ML, suggesting that the particles in the elevated layer were mixed into the ML"

We added an estimate of the ML height based on the Doppler lidar data as dashed line to the figure.

In Figure 1C the temperature soundings from Jokioinen show how a temperature inversion at the top of the previous day's ML remains at roughly the same altitude (2000-2500 m asl.) during the night and height of this inversion indicates the height of the residual layer.

Comment: L 168-171 : The NPF starts at 12:36 but the vertical particle flux show minimum values at 10:30 et 13:00. If aerosols are coming from the residual layer (around 1700m), the process is not instantaneous right ? So the NPF should be related to the minimums of Vertical particle flux occurring at 10:30 and 11:30. Can you estimate the vertical speed of the aerosols ? Is the aerosol speed playing a role in the NPF occurrence ? I would think that yes due to the fact that slow motion aerosol would have grown to much larger sizes ? Could you run the analysis also for non event days ? Is there a vertical wind speed threshold that need to be exceeded ? Also for other NPF cases linked to RL NPF events, Can you tell us more about the vertical particle flux patterns observed before the occurrence of NPF ? Is it different for each case ?

Answer: If the particles are formed at the top of the RL, disconnected from the ML, then the intensity of mixing in the ML would have no effect on the particle formation. If the particles are entrained into the ML then more intense mixing would transport the particles to the surface quicker and vice versa. Also if the ML remains quite shallow due to weak mixing it may be that the particle layer is not mixed down and remains aloft.

Buzorius et al. (2001) observed that the vertical particle flux was mostly negative during NPF events and the authors argued that the particles were probably formed aloft and mixed down.

In RL NPF we were looking for negative peak in particle flux when the nucleation mode particles were first observed. In other words the particle flux is most negative when the particles are observed for the first time since all the particles would be above the flux measurement setup and none below. As the particles are further mixed into the ML the number concentration difference above and below the flux measurement setup decreases and the particle flux becomes less negative.

Comment: Figure 6: I'm not sure what you plotted on this figure. The color code correspond to $dN/d\log D_p$ (cm⁻³). So is it a total concentration or is it from a specific bin ? It must be a specific bin and most probably within the fine diameter range due to the conclusions drawn. Could you please provide the percent of NPF event linked to aerosol formation in the upper layer ? Then you could use this result to justify the 75th percentile use.

Answer: The figure shows the median and the 75th percentile aerosol particle number size distribution as a function of altitude calculated from 2011-2018 flight data. We did not inspect all flight profiles during 2011-2018 for layers. However Väänänen et al. (2014) (reference in the manuscript) reported that for 2013-2014 campaigns 16/36 (~44%) profiles had a sub-25 nm particle layer. We added this number to the Introduction.

Comment: L52 : need to define ML

Answer: we added the following definition to the Introduction when we first mention the ML:

"Type of atmospheric boundary layer where turbulence tends to uniformly mix quantities such as aerosol particle concentrations."

Comment: L147 : In the aircraft data : not well said

Answer: We replaced it with "In the airborne measurements"

Comment: Figure 7 : Need to be more precise : - early morning of June 5th : 0 – 4h ?



Is there a reason why you choose that time to determine the Residual layer ? could you provide some stat for each cases of the delay between the moment when the Inversion layer reach the Residual layer and the moment when the NPF occurs at the ground ? That could be great to have as well the RL height, and the estimated speed of the aerosol.

Answer: We chose this sounding on Jun 5 because in the next sounding the RL was already mixed into the ML. In general we used the latest temperature profile where the top of the RL was visible. We added Table 1 that shows all this information (Fig. 2). We find this analysis is not accurate enough to estimate mixing speeds for the aerosol particles though.

Comment: L220 : So you found 8 cases out of ? That would be nice to see a table showing the number of days of observations, the number of events at the ground, the number of event linked to roll vortices, the number of event linked to the RL, and the number of event that are not yet related to anything. And precise the type of events (classic banana or burst of particles at higher diameter than 3nm ? Again here you said these cases were not observed at the same time : Could you provide a table with their main characteristic : Start time, duration, GR, diameter at time start ?

Answer: The campaign was 8 months Feb-Sep in 2014. We provide Table 1 (Fig. 2) for information on the specific cases. Since this particular analysis was to study the relationship between the mixing time of the RL top into ML and the appearance time of the nucleation mode particles. We did not think that classifying other types of NPF events would add much information.

Comment: L236 : please replace transported event by "transported event"

Answer: Fixed

Comment: L 246- 252 : could you provide the number and the percentage ?

Answer: We added these to the text

Comment: Reference that might be added to your manuscript : A lot of work have been done by the French group of the LaMP to study NPF events on the ground at an alti- tude site but also using aircraft measurements. You should cite some of them in your paper. Aircraft observations for links between altitude and NPF: Crumeyrolle et al 2010, Altitude site: Boulon, et al.: Investigation of nucleation events vertical extent: a long term study at two different altitude sites, Atmos. Chem. Phys., 11, 5625–5639, <https://doi.org/10.5194/acp-11-5625-2011>, 2011. C. Rose, et al., Frequent nucleation events at the high altitude station of Chacaltaya (5240 m a.s.l.), Bolivia, <https://doi.org/10.1016/j.atmosenv.2014.11.015>. H Venzac, et al - 2007 - Aerosol and ion number size distributions were measured at the top of the Puy de Dôme (1465 m above the sea level) for a three-month period. The goals were to investigate the vertical extent of nucleation in the atmosphere and the effect of clouds on nucleation. J. Boulon, et al. New particle formation and ultra- fine charged aerosol climatology at a high altitude site in the Alps (Jungfrauoch, 3580 m a.s.l., Switzer- land). Atmospheric Chemistry and Physics, European Geosciences Union, 2010, 10 (19), pp.9333-9349.

Also maybe look at that one : <https://www.mdpi.com/2072-4292/12/4/648>. It does also look at the impact of the dynamics on the nucleation events with a clear focus on the dynamics. You can actually see that the perturbation induced by flows at different altitude might also enhanced the possibility to observed NPF events. The turbulent fluxes occurring at each layer top is inducing favourable conditions to generate NPF events.

Answer: We thank the Referee for these references. We added more information to the Introduction regarding previous studies (see our answer to Referee #1). We added some of these studies there.

References

McNaughton, C. S., Clarke, A. D., Howell, S. G., Pinkerton, M., Anderson, B., Thornhill, L., Hudgins, C., Winstead, E., Dibb, J. E., Scheuer, E. and Maring, H.: Results from the

[Printer-friendly version](#)[Discussion paper](#)

DC-8 Inlet Characterization Experiment (DICE): Airborne Versus Surface Sampling of Mineral Dust and Sea Salt Aerosols, *Aerosol Science and Technology*, 41(2), 136–159, doi:10.1080/02786820601118406, 2007.

Buzorius, G., Rannik, Ü., Nilsson, D. and Kulmala, M.: Vertical fluxes and micrometeorology during aerosol particle formation events, *Tellus B*, 53(4), 394–405, doi:10.1034/j.1600-0889.2001.530406.x, 2001.

Interactive comment on *Atmos. Chem. Phys. Discuss.*, <https://doi.org/10.5194/acp-2020-923>, 2020.

ACPD

Interactive
comment

Printer-friendly version

Discussion paper



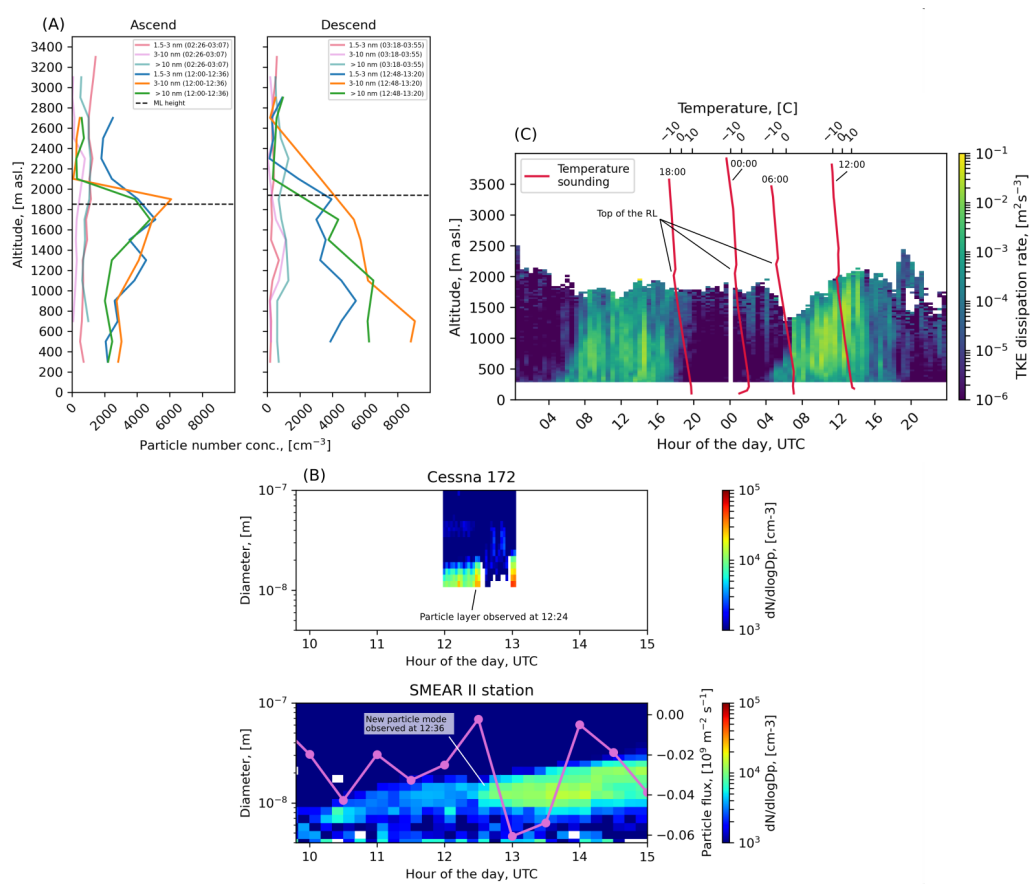


Fig. 1.

Table 1: rl_h = residual layer height during night or early morning (m asl), rl_ht = time when the rl_h was observed (time when the sounding was released, hour of the day, UTC), $mode_t$ = nucleation mode particle mode first appears (hour of the day, UTC), $mode_t1/mode_t2$ = nucleation mode particle mode appearance confidence interval (hour of the day, UTC), rl_t = new mixed layer reaches the top of the residual layer (hour of the day, UTC), rl_t1/rl_t2 = new mixed layer reaches the top of the residual layer confidence interval (hour of the day, UTC), bl_h = observed maximum height of the previous day's boundary layer (m asl.), dp = mean mode diameter for the newly appeared particle mode, when they first appear (nm), gr = growth rate calculated for the newly appeared particle mode (nm h^{-1}), pf = the value of the negative particle flux peak ($10^9 \text{ m}^{-2} \text{ s}^{-1}$).

date	rl_ht	rl_h	mode_t1	mode_t	mode_t2	rl_t1	rl_t	rl_t2	dp	bl_h	pf	gr
20140328	5.3	1100	8.5	9	9.5	5.5	7	8	20	1300	-0.25	2.28
20140331	7.6	2400	14	14.5	15	12	13.5	14	10	2200	-0.06	2.1
20140404	8.5	2200	10.5	11	11.5	10.5	11	11.5	8	2800	-0.04	1.39
20140409	5.5	1500	9	9.25	9.5	6	6.5	7	8	1800	-0.13	1.18
20140415	5.3	1600	14.5	14.25	15	12	13	14	11	1700	-0.18	1.94
20140422	0.0	1800	12	12.5	13	10.5	11	11.5	17	1900	-0.17	1.0
20140518	0.0	1500	9.5	10	10.5	8	8.5	9	13	1900	-0.11	2.91
20140705	5.3	1500	11	11.5	12	8.5	9	10	12	1700	-0.1	4.83

Fig. 2.

Aerosol particle formation in the upper residual layer

Authors:

Janne Lampilahti¹, Katri Leino¹, Antti Manninen², Pyry Poutanen¹, Anna Franck¹, Maija Peltola¹, Paula Hietala¹, Lisa Beck¹, Lubna Dada¹, Lauriane Quéléver¹, Ronja Öhrnberg¹, Ying Zhou³, Madeleine Ekblom¹, Ville Vakkari^{2,4}, Sergej Zilitinkevich^{1,2}, Veli-Matti Kerminen¹, Tuukka Petäjä^{1,5}, Markku Kulmala^{1,3,5}

Affiliations:

¹Institute for Atmospheric and Earth System Research / Physics, Faculty of Science, University of Helsinki, Helsinki, Finland.

²Finnish Meteorological Institute, Helsinki, Finland.

³Aerosol and Haze Laboratory, Beijing Advanced Innovation Center for Soft Matter Science and Engineering, Beijing University of Chemical Technology, Beijing, China.

⁴Atmospheric Chemistry Research Group, Chemical Resource Beneficiation, North-West University, Potchefstroom, South Africa.

⁵Joint International Research Laboratory of Atmospheric and Earth System Sciences, Nanjing University, Nanjing, China.

Correspondence to: Janne Lampilahti (janne.lampilahti@helsinki.fi)

Abstract: According to current estimates, atmospheric new particle formation (NPF) produces a large fraction of aerosol particles and cloud condensation nuclei in the earth's atmosphere, therefore having implications for health and climate. Despite recent advances, atmospheric NPF is still insufficiently understood in the [lower troposphere, especially above the mixed layer \(ML\). This upper parts of the boundary layer \(BL\). In addition, it is unclear how NPF in upper BL is related to the processes observed in the near-surface layer. The role of the topmost part of the residual layer \(RL\) in NPF is to a large extent unexplored.](#) This paper presents new results from co-located airborne and ground-based measurements in a boreal forest environment, showing that many NPF events (~42%) appear to start in the [topmost part of the upper RL](#). The freshly formed particles may be entrained into the growing mixed layer (ML) where they continue to grow in size, similar to the aerosol particles formed within the ML. The results suggest that in the boreal forest environment, NPF in the upper RL has an important contribution to the aerosol load in the BL.

1. Introduction

It has been estimated that atmospheric new particle formation (NPF) is responsible for most of the cloud condensation nuclei (CCN) in the atmosphere (Dunne et al., 2016; Gordon et al., 2017; Pierce and Adams, 2009; Yu and Luo, 2009). Aerosol-cloud interactions, in turn, have important but poorly-understood effects on climate (Boucher et al., 2013). Being a major source of ultrafine

41 aerosol particles in many environments (e.g. Brines et al., 2015; Posner and Pandis, 2015; Salma et
42 al., 2017; Yu et al., 2019), NPF may have implications for human health.

43 NPF has been observed in various environments and at various altitudes inside the troposphere. The
44 majority of NPF observations come from ground-based measurements (Kerminen et al., 2018;
45 Kulmala et al., 2004), which can be argued to represent NPF within the mixed layer (ML). ML is a
46 type of atmospheric BL where turbulence uniformly, especially vertically, mixes quantities like
47 aerosol particle concentrations. Measurements from aircrafts show that NPF is also common in the
48 upper free troposphere (FT) (e.g. Clarke and Kapustin, 2002; Takegawa et al., 2014). Entrainment
49 of particles formed in the upper FT was identified as an important source of CCN in the tropical
50 boundary layer (BL) (Wang et al., 2016; Williamson et al., 2019). Measurements from high-altitude
51 research stations also demonstrate that NPF frequently takes place in the FT, in these cases NPF was
52 often observed in BL air that was transported to the higher altitudes (Bianchi et al., 2016; Boulon et
53 al., 2011; Rose et al., 2017; Venzac et al., 2008).

54 |
55 When studying the vertical distribution of NPF in the lower troposphere one has to consider the
56 evolution and dynamics of the BL. Nilsson et al. (2001) found that the onset of turbulent mixing
57 correlated better with the onset of NPF at ground level than with the increase in solar radiation. The
58 authors gave several hypotheses to why this might be. One hypothesis was that NPF starts aloft,
59 either in the RL or in the inversion capping the shallow morning ML. As the turbulent mixing starts,
60 the newly formed particles would be transported down and observed at the ground-level.

61 |
62 Many observations have supported the hypothesis put forward by Nilsson et al. (2001). Größ et al.
63 (2018), Meskhidze et al. (2019) and Stanier et al. (2004) reported positive correlation between the
64 onset of NPF at ground level and the breakup of the morning inversion due to beginning of
65 convective mixing. Chen et al. (2018), Platis et al. (2015) and Siebert et al. (2004) used in situ
66 airborne measurements and observed that NPF started during the morning on the top of a shallow
67 ML capped by a temperature inversion at a few hundred meters above ground. The particles grew to
68 detectable nucleation mode (sub-25 nm) sizes aloft, and when the ML began to grow due to
69 thermally-driven convection, the particles were mixed downwards and observed at the ground-level
70 where they further continued to grow in size. Stratmann et al. (2003) observed newly formed
71 particles inside the RL disconnected from the shallow ML or the inversion that capped it.
72 Furthermore, Wehner et al. (2010) observed that NPF inside the RL was connected to turbulent
73 layers. On the other hand, Junkermann and Hacker (2018) attributed their observations of elevated

74 ultrafine particle layers at few hundred meter altitudes in the RL to flue gas emissions from
75 smokestacks with subsequent chemistry taking place during air mass transport over long distances.
76

77 The hypothesis proposed by Nilsson et al. (2001) was based on observations done in Hyytiälä,
78 Finland, which is a rural site surrounded by boreal forests and with very clean air. However, the
79 supporting evidence comes from measurements done in more polluted environments in Central
80 Europe and USA. Airborne measurements done over Hyytiälä have not found NPF on top of the
81 shallow morning ML or within the bulk of the RL, instead the NPF events seem to start within the
82 ML (Boy et al., 2004; Laakso et al., 2007; O'Dowd et al., 2009). This might be because in the more
83 polluted environments there are high enough concentrations of precursor vapors from
84 anthropogenic sources that NPF can be initiated in the morning inversion and/or within the bulk of
85 the RL. Interestingly, though, observations from Hyytiälä using a small instrumented airplane have
86 frequently found nucleation mode particle layers above the ML at a much higher altitude range of
87 ~1500-2800 m above ground and the explanation for these layers is not clear (Leino et al., 2019;
88 Schobesberger et al., 2013; Väänänen et al., 2016). For example Väänänen et al. (2016) found that
89 for the 2013-2014 airborne measurement campaigns 16/36 (~44%) profiles showed an elevated sub-
90 25 nm particle layer.
91

92 In this study we used co-located airborne and ground-based measurements to study nanoparticles
93 over a boreal forest in Hyytiälä, Finland. We aimed to characterize the elevated nucleation mode
94 particle layers that were a frequent observation in the previous studies. Specifically we were
95 looking at the following questions: (1) where in terms of atmospheric layers, how often and why do
96 these aerosol particle layer occur, and (2) how they are related to ground-based observations, and
97 what implications this has for data interpretation.

98 ~~**The majority of NPF observations come from ground-based measurements (Kerminen et al.,**~~
99 ~~**2018; Kulmala et al., 2004), which can be argued to represent NPF within the mixed layer**~~
100 ~~**(ML). Measurements from aircrafts (e.g. Clarke and Kapustin, 2002; Rose et al., 2017) and**~~
101 ~~**high-altitude research stations (e.g. Bianchi et al., 2016) demonstrate that NPF frequently**~~
102 ~~**takes place in the free troposphere (FT). Entrainment of particles formed in the upper FT was**~~
103 ~~**identified as an important source of CCN in the tropical boundary layer (BL) (Wang et al.,**~~
104 ~~**2016; Williamson et al., 2019).**~~

105
106 ~~**To what extent NPF happens in the lower FT and in the upper parts of the BL is not clear.**~~
107 ~~**Freshly formed particles were observed in the inversion capping a ML (Chen et al., 2018;**~~

108 ~~Platis et al., 2015; Siebert et al., 2004) and in turbulent layers inside the residual layer (RL)~~
109 ~~(Wehner et al., 2010). NPF was frequently observed in the lower FT over a megacity in a year-~~
110 ~~long campaign (Quan et al., 2017). Also Qi et al. (2019) reported NPF just above the ML over~~
111 ~~Yangtze River Delta. In the marine BL, sub-10 nm particles were observed in the entrainment~~
112 ~~zone above a cloud topped BL (Dadashazar et al., 2018). Layers of sub-10 nm particles,~~
113 ~~usually less than 500 m in thickness, were often observed in the lower FT over a boreal forest~~
114 ~~environment (Leino et al., 2019; Schobesberger et al., 2013; Väänänen et al., 2016). On the other~~
115 ~~hand, Junkermann and Hacker (2018) attributed their observations of ultrafine particle~~
116 ~~layers to flue gas emissions from stacks with subsequent chemistry taking place during air~~
117 ~~mass transport over long distances.~~

118 |
119 In this study we used co-located airborne and ground-based measurements to study NPF in the BL
120 over a boreal forest. We aimed to answer the following questions: (1) where, how often and why
121 does NPF take place in the upper parts of the BL, and (2) how the upper-BL NPF is related to
122 ground-based observations, and what implications this has for data interpretation.

124 **2. Materials and methods**

126 ***2.1. Airborne measurements***

127 |
128 We used data from airborne measurement campaigns conducted between 2011 and 2018 around
129 Hyytiälä, Finland. ~~Here we focused on data within 40 km radius from Hyytiälä.~~ Figure 1 shows the
130 data availability from these measurements. Most of the flights were carried out during spring and
131 early autumn because that is when NPF events are most common in Hyytiälä. ~~Here we focused on~~
132 ~~the data that was measured within a 40-km radius from Hyytiälä.~~ The measurement setups changed
133 slightly over the years. Detailed descriptions of the setups on board can be found ~~in our~~ previous
134 studies (Leino et al., 2019; Schobesberger et al., 2013; Väänänen et al., 2016).

135 |
136 The instrumented aircraft was a Cessna 172 operated from the Tampere-Pirkkala airport (ICAO:
137 EFTP). The sample air was collected through an outside inlet into a main sampling line that was
138 inside the aircraft's cabin. The forward movement of the aircraft during flight provided adequate
139 flow rate inside the main sampling line. The flow rate was maintained at 47 lpm by using a manual
140 valve. The instruments drew air from the main sampling line using core sampling inlets. The
141 necessary flow rate to the instruments was provided by pumps. The ~~flow rate in the main sampling~~

142 | ~~line corresponded to roughly isokinetic sampling at the core sampling inlets.~~ The airspeed was kept
143 | at 130 km/h during the measurement flights.

144

145 | The ~~aer-board~~ aerosol instruments on board considered in this study were an ultrafine condensation
146 | particle counter (uCPC, TSI, model: 3776), measuring the >3 nm particle number concentration at a
147 | 1-s time resolution, a particle size magnifier (PSM, Airmodus, model: A10) operated with a TSI
148 | 3010 CPC, measuring the >1.5 nm particle number concentration at a 1-s time resolution, and a
149 | custom-built scanning mobility particle sizer (SMPS) with a short Hauke type DMA and a TSI 3010
150 | CPC, measuring the aerosol number size distribution in the size range of 10-400 nm at a 2-min time
151 | resolution. In addition, basic meteorological data (temperature, relative humidity and pressure) and
152 | water vapor concentration from Licor Li-840 gas analyzer were used.

153

154 | Vertically, the measurement profiles extended approximately from 100 m to 3000 m above the
155 | ground. This altitude range covered the ML, RL and roughly 1 km of the FT (Figure 2). The
156 | measurement flights lasted about 2-3 hours and were flown mostly during the morning (~~~68:00-~~
157 | ~~102:00 UTC~~local time) and ~~the~~ afternoon (~~~113:00-146:00 UTC~~local time). Horizontally, the
158 | profiles were flown perpendicular to the mean wind in order to avoid the airplane's exhaust fumes.

159

160 | **2.2. Ground-based measurements**

161

162 | Comprehensive atmospheric measurements have been done at the SMEAR II station in Hyytiälä
163 | (61°50'40" N, 24°17'13" E, 180 m above sea level) since 1996 (Hari and Kulmala, 2005). The
164 | landscape around the site is flat and dominated by Scots pine forests, with small farms and lakes
165 | scattered nearby. The station represents typical rural background conditions.

166

167 | We used data from the BA ECC (Biogenic Aerosols–Effects on Clouds and Climate) campaign,
168 | which took place in Hyytiälä during Feb-Sep, 2014 (Petäjä et al., 2016), to study the relationship
169 | between BL evolution and NPF observed at the station. High spectral resolution lidar (HSRL)
170 | measurements and meteorological balloon soundings released every 4 hours by the U.S. Department
171 | of Energy ARM mobile facility allowed us to monitor the evolution of the BL (Nikandrova et al.,
172 | 2018).

173

174 | From the HSRL data we looked at the values of backscatter cross section in order to see the
175 | development of the ML during the day. The data were averaged into 30-m altitude bins and 10-min

176 temporal bins. The ground-based measurements during the BAECC campaign were also
177 supplemented by aircraft measurements using the instrumented Cessna. In case of missing
178 soundings, we also looked at the balloon soundings released from Jokioinen ~120 km south-west
179 from Hyytiälä (WMO: 02963).

180

181 The number size distribution of aerosol particles between 3 and 1000 nm was measured at the
182 station using a differential mobility particle sizer (DMPS, Aalto et al., 2001). A neutral cluster and
183 air ion spectrometer (NAIS, Airel Ltd., Mirme and Mirme, 2013) measured the number size
184 distribution of air ions and particles in the size ranges of 0.8-42 nm and 2-42 nm, respectively
185 (Manninen et al., 2009). The time resolutions of the DMPS and NAIS were 10 min and 4 min,
186 respectively. The vertical flux of particles >10 nm was measured by the eddy covariance method
187 from 23 m above ground, which is a couple of meters above the canopy (Buzorius et al., 2000). The
188 growth rates for aerosol particles were calculated using the log-normal mode fitting method
189 described in (Kulmala et al., 2012).

190

191 Vertical profiles of horizontal and vertical winds were measured with a Halo Photonics Stream Line
192 scanning Doppler lidar since year 2016. The Halo Photonics Stream Line is a 1.5 µm pulsed
193 Doppler lidar with a heterodyne detector and 30-m range resolution, and the minimum range of the
194 instrument is 90 m (Pearson et al., 2009). At Hyytiälä, a vertical stare of 12 beams and integration
195 time of 40 s per beam is scheduled every 30 min, whereas the other scan types operated during the
196 30-min measurement cycle were not utilized in this study. The lidar data were corrected for a
197 background noise artifact (Vakkari et al., 2019). The turbulent kinetic energy (TKE) dissipation rate
198 was calculated from the vertical stare according to the method by O'Connor et al. (2010) with a
199 signal-to-noise-ratio threshold of 0.001 applied to the data. Data availability is limited by relatively
200 low aerosol concentration at Hyytiälä, but TKE dissipation rate can be retrieved on most days up to
201 the top of the BL.

202 ~~The number size distribution of aerosol particles between 3 and 1000 nm was measured at the~~
203 ~~station using a differential mobility particle sizer (DMPS, Aalto et al., 2001). A neutral cluster~~
204 ~~and air ion spectrometer (NAIS, Airel Ltd., Mirme and Mirme, 2013) measured the number~~
205 ~~size distribution of air ions and particles in the size ranges of 0.8-42 nm and 2-42 nm,~~
206 ~~respectively (Manninen et al., 2009). The time resolutions of the DMPS and NAIS were 10 min~~
207 ~~and 4 min, respectively. The vertical flux of particles >10 nm was measured by the eddy~~
208 ~~covariance method from 23 m above ground, which is a couple of meters above the canopy~~
209 ~~(Buzorius et al., 2000).~~

210 |
211 | Vertical profiles of horizontal and vertical winds were measured with a Halo Photonics
212 | Stream Line scanning Doppler lidar since year 2016. The Halo Photonics Stream Line is a 1.5-
213 | µm pulsed Doppler lidar with a heterodyne detector and 30-m range resolution, and the
214 | minimum range of the instrument is 90 m (Pearson et al., 2009). At Hyytiälä, a vertical stare
215 | of 12 beams and integration time of 40 s per beam is scheduled every 30 min, whereas the
216 | other scan types operated during the 30-min measurement cycle were not utilized in this
217 | study. The lidar data were corrected for a background noise artifact (Vakkari et al., 2019).
218 | The turbulent kinetic energy (TKE) dissipation rate was calculated from the vertical stare
219 | according to the method by O'Connor et al. (2010) with a signal-to-noise-ratio threshold of
220 | 0.001 applied to the data. Data availability is limited by relatively low aerosol concentration at
221 | Hyytiälä, but TKE dissipation rate can be retrieved on most days up to the top of the BL.

222 | _____

223 | **3. Results and discussion**

224 |

225 | In the airborne measurements we frequently observed a layer of nucleation mode (sub-25 nm)
226 | particles above the ML. First we introduce how the phenomenon was observed in the airborne and
227 | ground-based measurements using two case studies. Then we show that sub-25 nm particle layers
228 | occurred in the topmost part of the RL by studying the average vertical profile of particle number-
229 | size distribution and temperature from the airplane. Then we associate the nucleation mode particles
230 | in the upper RL to a specific signal in the ground-based measurements and use the observations at
231 | the SMEAR II station to gather long-term statistics. All times are reported in UTC.

232 | In the aircraft data we frequently observed a layer of nucleation mode (sub-25 nm) particles above-
233 | the ML. First we introduce how the phenomenon was observed in the airborne and ground-based
234 | measurements using a case study. Then we show that the particle layers occurred in the topmost part
235 | of the RL, by studying the average vertical profile of particle number-size distribution and
236 | temperature as well as the BAEC data. Finally, by using the BAEC data, we associate the
237 | nucleation mode particles in the upper RL to a specific signal in the ground-based measurements-
238 | and use the observations at the SMEAR II station to gather long-term statistics.

239 |

240 | ***3.1 Case study: May 2, 2017***

241 |

242 | On May 2, 2017 during the measurement airplane's ascend over Hyytiälä we observed an increased
243 | number concentration of 3-10 nm (N_{3-10}) and 1.5-3 nm ($N_{1.5-3}$) particles, approximately between

244 1200 and 2000 m above sea level (asl), in the top parts of the ML (Figure 3A). The lower edge of
245 the aerosol particle layer was observed at 12:24. Within the particle layer the maximum $N_{1.5-3}$ was
246 $\sim 5000 \text{ cm}^{-3}$ and N_{3-10} was $\sim 6000 \text{ cm}^{-3}$. Below the particle layer $N_{1.5-3}$ and N_{3-10} were $\sim 2200 \text{ cm}^{-3}$.
247 Above the layer N_{3-10} dropped to $\sim 200 \text{ cm}^{-3}$. This low number concentration indicates that the
248 airplane was measuring in the RL/FT. The $N_{1.5-3}$ dropped to $\sim 2000 \text{ cm}^{-3}$ and further down to ~ 200
249 cm^{-3} during the descend. The PSM probably had some problems stabilizing at higher altitudes. The
250 bottom of the particle layer was well within the ML and the particles were in the process of being
251 mixed into the rest of the ML.

252
253 During the descend the airplane entered back into the ML at 12:56 and the $N_{1.5-3}$ and N_{3-10} were
254 increased throughout the ML, indicating that the particle layer was further mixed into the ML. The
255 $N_{1.5-3}$ was around 4000 cm^{-3} and N_{3-10} increased from 4000 cm^{-3} to around 8000 cm^{-3} towards the
256 surface. On the same day, an early morning flight before the sunrise was also performed (Figure
257 3A). During this flight no elevated aerosol particle layer was observed and the number
258 concentrations were quite uniform with altitude in the different size ranges, staying below 1500 cm^{-3} .
259 .

260
261 Roughly 10 min after the aerosol particle layer was first observed from the airplane during the
262 ascend, a new particle mode with similar-sized particles (geometric mean mode diameter about 10
263 nm) appeared at the ground-level at 12:36 (Figure 3B). The appearance of this new particle mode
264 was characterized by a negative peak in the vertical particle flux, further suggesting that the
265 particles were mixed down from aloft. The new particle mode continued to grow for several hours
266 despite the airmass moving over Hyytiälä, indicating a large horizontal source area for the particles.
267 At the ground level a new particle mode with lower number concentration coupled with negative
268 particle flux also appeared at around 10:00. It may be that these particles were also mixed down
269 from higher altitudes, but in the absence of airplane measurements during that time, we cannot be
270 sure.

271
272 The airmasses came from the Arctic Ocean over northern Scandinavia. They went over the west
273 coast of Finland where there are known pollution sources, however in Hyytiälä the SO_2 and CO
274 levels remained low all day ($\sim 0.025 \text{ ppb}$ and $\sim 115 \text{ ppb}$ for SO_2 and CO, respectively). Even when
275 the particles were observed at the surface no increase in pollutant concentrations was observed.
276 Pollution released into the night time RL from elevated sources such as flue gas stacks would be
277 expected to form layers at lower altitudes, below few hundred meters. If the pollution is released

278 during daytime, it is expected to be uniformly mixed into the ML and stay like that in the RL
279 (Junkermann and Hacker, 2018). The likely explanation for sub-10 and sub-3 nm particles at this
280 altitude is NPF.

281 |
282 In order to study the atmospheric layers in the lower troposphere we plotted the TKE dissipation
283 rate calculated from the Doppler lidar measurements during May 1-2, 2017 and temperature
284 soundings from Jokioinen (Figure 3C). In the Doppler lidar measurements, the increase in the TKE
285 dissipation rate reveals the development of the ML on both days. On May 1, 2017 the ML reached
286 roughly 1900 m asl. The temperature sounding at 18:00 shows that this mixed layer was capped by
287 a thermal inversion at about 2000 m asl. In the two subsequent soundings during the night the
288 inversion stayed at roughly the same altitude and marked the top of the RL. In the temperature
289 sounding on May 2, 2017 at 12:00 only one inversion is observed at about 1900 m asl suggesting
290 that at this point the RL was already mixed into the growing ML. The lidar measurement agrees that
291 on May 2, 2017 the ML reached 1900 m asl around 12:00. About 25 min later the aerosol particle
292 layer was observed from the Cessna.

293 | 294 ***3.2 Case study: May 19, 2018***

295 |
296 On May 19, 2018 another case of nucleation mode particles mixing down into the ML was
297 observed. Figure 4A shows that during the airplane's ascend the lower edge of the particle layer was
298 observed at ~1200 m asl and the top of the layer was at 2000 m asl. The N_{3-10} increased in the layer
299 from ~1000 cm^{-3} up to ~10000 cm^{-3} . When the airplane descended back into the ML the N_{3-10} was
300 increased to around 6000 cm^{-3} throughout the ML, suggesting that the particle layer was mixed into
301 the ML. The air masses arrived from a similar sector as in the May 2, 2017 case (Arctic Ocean over
302 northern scandinavia). SO_2 and CO concentrations in Hyttiälä remained low when the particles
303 were mixed down (~0.05 ppb and ~127 ppb for SO_2 and CO, respectively).

304 |
305 Figure 4B shows particle number size distribution measurements from the measurement airplane
306 and from the field station. The particle layer was observed as increased number concentrations in
307 the smallest size channels of the SMPS at 9:00 before the airplane flew above the ML. Roughly 20
308 minutes later a similar-sized particle mode appeared in the ground-based data. For this day there
309 were no particle flux data. The new particle mode continued to grow larger inside the ML for
310 several hours.

311 |

312 Figure 4C shows the TKE dissipation rate on May 18-19, 2018 from Hyytiälä and temperature
313 soundings from Jokioinen. On May 18, 2018 the ML went up to 2500 m asl in Hyytiälä. The
314 Jokioinen soundings show that at 6:00 the top of the RL was at about 1800 m asl, marked by the
315 subsiding inversion left from the previous day's ML. The particle layer mixed down from
316 approximately 2000 m asl.

317 |
318 ~~*On May 2 during the measurement airplane's ascend over Hyytiälä, we observed a layer of*~~
319 ~~*freshly formed aerosol particles approximately between 1200 and 2000 m above the ground, in*~~
320 ~~*the top parts of the ML (Figure 3). The layer had increased number concentrations of sub-20 nm*~~
321 ~~*and sub-3 nm particles. The small size of the particles suggests that they were recently formed in*~~
322 ~~*the atmosphere. The lower edge of the aerosol particle layer was observed at 12:24 UTC. The*~~
323 ~~*airplane entered back into the ML at 12:56 UTC and at this point there were no signs of the*~~
324 ~~*particle layer, but the particle number concentration had increased inside the ML. On the same*~~
325 ~~*day, an early morning flight before the sunrise was also performed. During this flight no elevated*~~
326 ~~*particle layer was observed below 3000 m, suggesting that this particle layer had been formed*~~
327 ~~*after the sunrise. The air masses came from a non-polluted sector over the Arctic Ocean and*~~
328 ~~*northern Scandinavia.*~~

329 ~~After the aerosol layer was observed from the airplane during the ascend, a new particle mode with~~
330 ~~a geometric mean diameter of about 10 nm suddenly appeared at the ground-level at 12:36 (Figure~~
331 ~~4). The appearance of this new particle mode was characterized by a negative peak in the vertical~~
332 ~~particle flux, suggesting that the particles had been mixed down from aloft.~~

333 |
334 ~~We then studied the vertical profiles of meteorological quantities measured on board the Cessna on~~
335 ~~May 2, and the turbulent kinetic energy (TKE) dissipation rate calculated from the Doppler lidar~~
336 ~~measurements during May 1-2 (Figure 5). In the Doppler lidar measurements, the increase in the~~
337 ~~TKE dissipation rate clearly reveals the development of the ML on both days. On May 1 the ML~~
338 ~~reached roughly 1700 m above the ground, while on May 2 the first potential temperature profile~~
339 ~~measured on board the Cessna revealed the presence of a stable layer (upper RL) at roughly the~~
340 ~~same altitude. This matches with the height of the aerosol particle layer in Figure 3. The Doppler~~
341 ~~lidar measurements further show that on May 2 the ML reached this height around the noon UTC,~~
342 ~~which is when the particle layer was observed to be mixing down. This leads us to hypothesize that~~
343 ~~NPF was taking place in the upper RL.~~

344 **3.42 Evidence of NPF in the upper RL based on long-term measurements**

345 |

346 In the two case studies above the aerosol particle layer mixed down from approximately the altitude
347 where the top of the RL was. In order to study this connection further we analyzed the airborne data
348 measured during 2011-2018. In Figure 5 we plotted the median and 75th percentile number size
349 distributions measured on board the aircraft as a function of altitude during NPF event days (65
350 days out of 130 measurement days) between 07:00 and 10:00 UTC. This is the time window when
351 the morning measurement flight was usually done. NPF event days are characterized by a new
352 growing particle mode appearing in the sub-25 nm size range (Dal Maso et al., 2005). If aerosol
353 formation in the upper RL occurs on less than half of the NPF event days, it might not be visible in
354 the median plot, but might still appear in the 75th percentile plot.

355 ~~We analyzed the airborne data measured during 2011-2018. We plotted the median and 75th-~~
356 ~~percentile number size distributions measured on board the aircraft as a function of altitude during~~
357 ~~NPF event days (65 days out of 130 measurement days) between 09:00 and 12:00 (Figure 6). NPF-~~
358 ~~event days are characterized by a new growing particle mode appearing in the sub-25 nm size range~~
359 ~~(Dal Maso et al., 2005). If aerosol formation in the upper RL occurs on less than half of the NPF-~~
360 ~~event days, it might not be visible in the median plot, but might still appear in the 75th-percentile~~
361 ~~plot.~~

363 Interestingly, in the 75th percentile plot a layer of nucleation mode particles is observed at 2500-
364 3000 m above sea level. This altitude range is well above the still growing ML at 07:00-10:00. We
365 wanted to know if the elevated particle layer was associated with a temperature inversion, since the
366 RL is commonly capped by such an inversion (Stull, 1988). In Figure 5 we plotted the mean
367 temperature profile from the flights when the N_{10-25} in 2000-3000 m altitude range exceeded the 75th
368 percentile N_{10-25} value (18 days).

370 The temperature profile shows an inversion base at 2500 m and this is likely where on average the
371 top of the RL was. The reason for the unusually deep RL is probably that the NPF event days tend
372 to be sunny spring days and the ML can grow exceptionally high, which also leads to a deep RL.
373 Our finding is in line with previous observations by Schobesberger et al. (2013) who measured
374 nucleation mode particles close to an elevated temperature inversion above the ML on multiple
375 measurement flights over southern Finland.

377 **Interestingly, in the 75th percentile plot a layer of nucleation mode particles is observed at**
378 **2500-3000 m above sea level. In the mean temperature profile, an inversion is observed at the**

379 ~~same altitude level. The ML and RL are commonly capped by temperature inversions (Stull,~~
380 ~~1988).~~

381 ~~In this case, the inversion is likely where on average the top of the RL was, since the the top of the~~
382 ~~ML was well below this altitude. The probable reason for the unusually deep RL is that the NPF~~
383 ~~event days tend to be sunny spring days and the ML can grow exceptionally high, which also leads~~
384 ~~to a very deep RL. The vertical profile of particle number size distribution supports the idea that~~
385 ~~NPF was taking place in the upper RL.~~

386 **3.53 Connection between NPF in the upper RL and ground-based observations**

387

388 With the BAecc dataset we wanted to investigate whether the sudden appearance of nucleation
389 mode particles with downward particle flux was associated with the ML reaching the upper RL.
390 This would not only further test the hypothesis that NPF happens in the topmost part of the RL, but
391 also provide us with a condition~~tool~~ to identify upper RL NPF from the ground-based data alone.

392

393 We looked for cases where a new particle mode suddenly appeared in the nucleation mode size
394 range during the daytime and the first observation of these particles was associated with a negative
395 peak in particle flux. We noted the times when the particles first appeared, and also estimated a
396 confidence interval of the observation. Then we checked if we could find out the height of the RL
397 from balloon soundings or the Cessna flights. We looked for an elevated temperature inversion that
398 was roughly at the same altitude as the previous day's maximum ML height, which was determined
399 from HSRL and/or sounding. We noted the base height of the temperature inversion and took this as
400 the top of the RL. Then we followed the height of the new ML from the HSRL measurements and
401 noted the time when the ML reached the inversion base, also estimating a confidence interval.

402 Figure 6 illustrates an example for this procedure.

403

404 ~~We looked for cases where a new particle mode suddenly appeared in the nucleation mode size~~
405 ~~range during the daytime and the appearance of the particles was associated with a downward~~
406 ~~particle flux. We noted the times when the particles first appeared, and also estimated a confidence~~
407 ~~interval of the observation. Then we checked if we could find out the height of the RL from balloon~~
408 ~~soundings or the Cessna flights. We looked for an elevated temperature inversion that was roughly~~
409 ~~at the same altitude as the ML of the previous day had reached. We noted the base height of the~~
410 ~~temperature inversion and took this as the top of the RL. Then we followed the height of the new~~
411 ~~ML from the HSRL measurements and noted the time when the ML reached the inversion base, also~~
412 ~~estimating a confidence interval. Figure 7 illustrates an example for this procedure.~~

413 We found 8 cases during the campaign where the analysis could be fully carried out and they are
414 summarized in Table 1. Figure 78 shows a ~~strong~~ positive correlation between the new particle
415 mode appearance time and the time when the ML reached the top of the RL. This suggests that the
416 suddenly appearing nucleation mode particles were entrained into the ML from the upper RL. We
417 found only a weak positive correlation between the new particle mode appearance time and the
418 geometric mean diameter of particles in the new mode at the moment they were first observed. This
419 is probably explained by the NPF starting at different times during the day and variability in growth
420 rates, coupled with the small sample size. The mean growth rate of the appearing particle modes at
421 the was 2.2 nm h⁻¹ which is similar to 2.5 nm h⁻¹ reported by Nieminen et al. (2014) for 3-25 nm
422 particles during NPF events in Hyytiälä.

424 The time that the ML reaches the upper RL depends on the height of the RL, which in turn depends
425 on the height of the ML on the previous day and the rate at which the top of the RL subsides. The
426 mixing time also depends on the rate at which the ML on the day of interest grows. For example on
427 March 28, 2014 the ML height on the previous day and the RL height during the night were 1300 m
428 and 1100 m, respectively. On April 4, 2014 the corresponding numbers were 2800 m and 2200 m.
429 Because of this on March 28, 2014 the ML reached the upper RL much earlier at ~7:00 compared to
430 April 4, 2014 when the ML reached the upper RL at ~11:00. For example on April 15, 2014 the ML
431 grew slowly in the morning due to presence of low clouds that limited convection. Because of this
432 the ML reached the top of the RL relatively late at 13:00.

434 In a well-mixed layer we would expect the entrained particles to reach the surface in less than an
435 hour (Stull, 1988). If the BL was stratified the particles could reach the surface at very different
436 rates which might significantly distort the results in Figure 7. The balloon soundings indicate that
437 the MLs in the 8 cases were well-mixed since the potential temperature profiles calculated from
438 soundings released around noon and late afternoon were almost constant up to the top of the ML
439 (see example profile in Figure 6).

441 **3.64 Implications for classifying NPF events**

443 Previous studies that classified NPF events observed in Hyytiälä have collected statistics on the
444 occurrence of suddenly appearing particle modes. ~~For example~~ Buenrostro Mazon et al., (2009)
445 classified the so-called undefined days between 1996-2006 from Hyytiälä. The undefined days are
446 days that do not fit the NPF event or the nonevent day classes (Dal Maso et al., 2005). One category

447 the authors used was collected statistics on “tail events” where a new particle mode appears at
448 particle diameters greater than 10 nm and grows for several hours. The authors found that 26% of
449 NPF events were tail events (assuming that tail events were also NPF events). Dada et al., (2018)
450 collected statistics on “transported events” where elevated number concentration of 7-25 nm
451 particles persisted for more than 1.5 hours, but no elevated number concentrations at smaller
452 particle sizes were observed. It was found that ~36% of the NPF events observed for over 10 years
453 in Hyytiälä were “transported events”. They occurred especially when the conditions inside the ML
454 were less favorable for nucleation.

455
456 Here we found cases in the SMEAR II data between 2013 and 2017, in which a new growing
457 particle mode suddenly, without continuous growth from smallest detectable sizes (3 nm), appears
458 in the nucleation mode and is associated with a negative peak in the vertical particle flux. We also
459 noted cases where a new particle mode appears with a continuous growth from the smallest
460 detectable sizes. Based on the previous analysis we assume that in the former case NPF took place
461 in the upper RL and in the latter case inside the ML. The analysis included 1750 days.

462
463 The monthly fractions of the different cases are shown in Figure 8. We found that NPF within the
464 ML occurred on 13% (234/1750) of all the days and NPF in the upper RL on 7% (117/1750) of all
465 the days. During spring (Mar-May) the corresponding percentages were 31% (132/431) and 17%
466 (74/431). On many days NPF took place both in the upper RL and within the ML (4% or 74/1750 of
467 all days and 12% or 53/431 of spring days). According to this analysis, NPF in the upper RL
468 constitutes 42% (117/277) of the NPF event days in Hyytiälä.

469
470 The monthly distribution of upper RL NPF events follows the distribution of ML NPF events, with
471 a peak during spring (Mar-May). This is well in line with previous studies that classified NPF
472 events in Hyytiälä (Dal Maso et al., 2005; Nieminen et al., 2014). This makes sense since the
473 conditions favoring ML NPF would also favor upper RL NPF. However, Buenrostro Mazon et al.
474 (2009) and Dada et al (2018) found that the tail events and transported events had a peak during the
475 summer months (Jun-Aug).

476
477 On 16% of the NPF event days NPF only took place in the upper RL but not in the ML. This
478 number is smaller than the 36% found by Dada et al. (2018) for transported events and the 26%
479 found by Buenrostro Mazon et al. (2009) for tail events. This might be because we restricted to
480 cases where a negative peak in particle flux was associated with the appearance of nucleation mode

481 particles. For example, a case where the particles were horizontally advected to the measurement
482 site would not be expected to cause a negative peak in the particle flux and therefore would not be
483 classified as upper RL NPF.

485 **3.7 Proposed explanation for the results**

486
487 The monthly fractions of the different cases are shown in Figure 9. We found that NPF within the
488 ML occurred on 13% of all the days and NPF in the upper RL on 7% of all the days. During spring
489 (Mar-May) the corresponding percentages were 31% and 17%. On many days NPF took place both
490 in the upper RL and within the ML. According to this analysis, NPF in the upper RL constitutes
491 42% of the NPF event days in Hyytiälä. Moreover, on 16% of the NPF event days NPF only took
492 place in the upper RL but not in the ML.

493 The gaseous precursors involved in NPF may end up in the upper RL because of mixing from the
494 surface during the previous day (e.g. organic vapors emitted from the forest or sulfuric acid,
495 ammonia and amines originating from human activities) or because of long-range transport in the
496 FT (e.g. iodine oxides from the ocean).

497
498 Many factors favor NPF at higher altitudes, including enhanced photochemistry, reduced sinks and
499 reduced temperature. However, the NPF inducing features of the upper RL are probably linked to
500 the mixing that takes place in the interface between the RL and FT, since this is the place where
501 NPF seems to be limited to. Nilsson and Kulmala, (1998) found that mixing two air parcels with
502 different initial temperatures and precursor vapor concentrations can lead to a considerable increase
503 in the nucleation rate. Therefore mixing air from the RL and FT over the inversion, where the
504 precursors are present in one of the layers, could lead to aerosol particle formation. Another
505 possibility is that the RL and the FT contain different precursor vapors that cannot form particles on
506 their own, however when the vapors are mixed in the interface between the two layers NPF occurs.

507
508 If the growing ML reaches the upper RL, the newly formed particles will be mixed downwards into
509 the ML where they continue to grow in size as low-volatility vapors present in the ML are able to
510 condense onto these particles. The processes are illustrated in Figure 9. In case the particles will not
511 be mixed down, they may persist in the FT for a longer time period and possibly have stronger
512 contribution to cloud formation.

513 **Many factors favor NPF at higher altitudes, including enhanced photochemistry, reduced sinks**
514 **and reduced temperature. However, the unique NPF inducing features of the upper RL are**

515 ~~*probably linked to the mixing that takes place in the interface between RL and FT. For example*~~
516 ~~*Nilsson and Kulmala, (1998) found that mixing two air parcels with different initial temperatures*~~
517 ~~*and precursor vapor concentrations can lead to a considerable increase in the nucleation rate.*~~

518 |
519 If the new ML reaches the upper RL, particles formed originally in the RL will be mixed into the
520 ML where they continue to grow in size as low-volatility vapors present in the ML are able to
521 condense onto these particles. The processes are illustrated in Figure 10. In case the particles will
522 not be mixed down, they may persist in the FT for a longer time period and possibly have stronger
523 contribution to cloud formation.

524 | 525 **4. Conclusions**

526
527 We measured aerosol particles, trace gases and meteorological parameters on board an instrumented
528 Cessna 172 over a boreal forest in Hyytiälä, Finland. The airborne data was complemented by the
529 continuous, comprehensive ground-based measurements at the SMEAR II station.

530
531 We found multiple evidence that NPF frequently takes place in the topmost part of the RL. This is
532 likely related to the ~~unique thermodynamic conditions present in this layer due to~~ mixing between
533 RL and FT air. We estimate that NPF in the upper RL occurs on 42% of the NPF event days in
534 Hyytiälä. Our results provide new information on NPF in the BL and they should be taken into
535 account when interpreting and analyzing ground-based as well as airborne measurements of aerosol
536 particles.

537
538 **Data availability:** The particle flux and DMPS data can be accessed from [https://avaa.tdata.fi/web/](https://avaa.tdata.fi/web/smart/smea)
539 [smart/smea](https://avaa.tdata.fi/web/smart/smea) (Junninen et al., 2009; last access: Oct 1, 2020). The BAEC HSRL and radiosonde
540 data is available from <https://adc.arm.gov/discovery/> (Bambha et al., 2014; Keeler et al., 2014); last
541 access: Oct 1, 2020). The Jokioinen soundings can be accessed using the Finnish Meteorological
542 Institute's open data service <https://en.ilmatieteenlaitos.fi/open-data> (last access: Oct 1, 2020). The
543 ERA5 dataset can be accessed from <https://cds.climate.copernicus.eu/cdsapp#!/home> (last access:
544 May 6, 2020). The rest of the data was gathered into a dataset that can be accessed from
545 <https://zenodo.org/record/4063662#.X3cHQnUzY88> (Lampilahti et al., 2020; last access: Oct 2,
546 2020).

547

548 **Author contribution:** JL, KL, AM, PP, AF, MP, PH, LD and LJQ conducted the airborne
549 measurements in 2017. PP wrote processing script for the airborne data. RÖ classified the SMEAR
550 II data for NPF events between 2013-2017. LB contributed to the data analysis. YZ and ME
551 analyzed the airborne data between 2011-2018. VV provided the Doppler lidar data. JL prepared the
552 manuscript with contributions from all co-authors.

553

554 **Acknowledgements:** This project has received funding from the ERC advanced grant No. 742206,
555 the European Union's Horizon 2020 research and innovation program under grant agreement No.
556 654109, the Academy of Finland Center of Excellence project No. 272041. SZ acknowledges
557 support from the Academy of Finland grant 314 798/799. We thank Erkki Järvinen and the pilots at
558 Airspark Oy for operating the research airplane and we are grateful for their hospitality and
559 helpfulness.

560

561 **References**

562

Aalto, P., Hämeri, K., Becker, E., Weber, R., Salm, J., Mäkelä, J. M., Hoell, C., O'Dowd, C. D., Hansson, H.-C., Väkevä, M., Koponen, I. K., Buzorius, G. and Kulmala, M.: Physical characterization of aerosol particles during nucleation events, *Tellus B*, 53(4), 344–358, doi:10.3402/tellusb.v53i4.17127, 2001.

Bambha, R., Eloranta, E., Garcia, J., Ermold, B. and Goldsmith, J.: High Spectral Resolution Lidar (HSRL), *Atmospheric Radiat. Meas. ARM User Facil.*, doi:10.5439/1025200, 2014.

Bianchi, F., Tröstl, J., Junninen, H., Frege, C., Henne, S., Hoyle, C. R., Molteni, U., Herrmann, E., Adamov, A., Bukowiecki, N., Chen, X., Duplissy, J., Gysel, M., Hutterli, M., Kangasluoma, J., Kontkanen, J., Kürten, A., Manninen, H. E., Münch, S., Peräkylä, O., Petäjä, T., Rondo, L., Williamson, C., Weingartner, E., Curtius, J., Worsnop, D. R., Kulmala, M., Dommen, J. and Baltensperger, U.: New particle formation in the free troposphere: A question of chemistry and timing, *Science*, aad5456, doi:10.1126/science.aad5456, 2016.

Boucher, O., Randall, D., Artaxo, P., Bretherton, C., Feingold, G., Forster, P., Kerminen, V.-M., Kondo, Y., Liao, H., Lohmann, U., Rasch, P., Satheesh, S. K., Sherwood, S., Stevens, B. and Zhang, X. Y.: Clouds and Aerosols, in *Climate Change 2013: The Physical Science Basis. Contribution of Working Group I to the Fifth Assessment Report of the Intergovernmental Panel on Climate Change*, edited by T. F. Stocker, D. Qin, G.-K. Plattner, M. Tignor, S. K. Allen, J. Boschung, A. Nauels, Y. Xia, V. Bex, and P. M. Midgley, pp. 571–658, Cambridge University Press, Cambridge, United Kingdom and New York, NY, USA. [online] Available from: www.climatechange2013.org, 2013.

[Boulon, J., Sellegri, K., Hervo, M., Picard, D., Pichon, J.-M., Fréville, P. and Laj, P.: Investigation of nucleation events vertical extent: a long term study at two different altitude sites, *Atmospheric Chem. Phys.*, 11\(12\), 5625–5639, doi:https://doi.org/10.5194/acp-11-5625-2011, 2011.](https://doi.org/10.5194/acp-11-5625-2011)

[Boy, M., Petäjä, T., Dal Maso, M., Rannik, Ü., Rinne, J., Aalto, P., Laaksonen, A., Vaattovaara, P., Joutsensaari, J., Hoffmann, T., Warnke, J., Apostolaki, M., Stephanou, E. G., Tsapakis, M.,](https://doi.org/10.5194/acp-11-5625-2011)

[Kouvarakis, A., Pio, C., Carvalho, A., Römpf, A., Moortgat, G., Spirig, C., Guenther, A., Greenberg, J., Ciccioli, P. and Kulmala, M.: Overview of the field measurement campaign in Hyytiälä, August 2001 in the framework of the EU project OSOA, *Atmospheric Chem. Phys.*, 4\(3\), 657–678, doi:10.5194/acp-4-657-2004, 2004.](#)

Brines, M., Dall'Osto, M., Beddows, D. C. S., Harrison, R. M., Gómez-Moreno, F., Núñez, L., Artíñano, B., Costabile, F., Gobbi, G. P., Salimi, F., Morawska, L., Sioutas, C. and Querol, X.: Traffic and nucleation events as main sources of ultrafine particles in high-insolation developed world cities, *Atmospheric Chem. Phys.*, 15(10), 5929–5945, doi:https://doi.org/10.5194/acp-15-5929-2015, 2015.

Buenrostro Mazon, S., Riipinen, I., Schultz, D. M., Valtanen, M., Maso, M. D., Sogacheva, L., Junninen, H., Nieminen, T., Kerminen, V.-M. and Kulmala, M.: Classifying previously undefined days from eleven years of aerosol-particle-size distribution data from the SMEAR II station, Hyytiälä, Finland, *Atmospheric Chem. Phys.*, 9(2), 667–676, doi:https://doi.org/10.5194/acp-9-667-2009, 2009.

Buzorius, G., Rannik, Ü., Mäkelä, J. M., Keronen, P., Vesala, T. and Kulmala, M.: Vertical aerosol fluxes measured by the eddy covariance method and deposition of nucleation mode particles above a Scots pine forest in southern Finland, *J. Geophys. Res. Atmospheres*, 105(D15), 19905–19916, doi:10.1029/2000JD900108, 2000.

Chen, H., Hodshire, A. L., Ortega, J., Greenberg, J., McMurry, P. H., Carlton, A. G., Pierce, J. R., Hanson, D. R. and Smith, J. N.: Vertically resolved concentration and liquid water content of atmospheric nanoparticles at the US DOE Southern Great Plains site, *Atmospheric Chem. Phys.*, 18(1), 311–326, doi:https://doi.org/10.5194/acp-18-311-2018, 2018.

Clarke, A. D. and Kapustin, V. N.: A Pacific Aerosol Survey. Part I: A Decade of Data on Particle Production, Transport, Evolution, and Mixing in the Troposphere, *J. Atmospheric Sci.*, 59(3), 363–382, doi:10.1175/1520-0469(2002)059<0363:APASPI>2.0.CO;2, 2002.

Dada, L., Chellapermal, R., Buenrostro Mazon, S., Paasonen, P., Lampilahti, J., Manninen, H. E., Junninen, H., Petäjä, T., Kerminen, V.-M. and Kulmala, M.: Refined classification and characterization of atmospheric new-particle formation events using air ions, *Atmospheric Chem. Phys.*, 18(24), 17883–17893, doi:https://doi.org/10.5194/acp-18-17883-2018, 2018.

[Dadashazar, H., Braun, R. A., Crosbie, E., Chuang, P. Y., Woods, R. K., Jonsson, H. H. and Sorooshian, A.: Aerosol characteristics in the entrainment interface layer in relation to the marine boundary layer and free troposphere, *Atmospheric Chem. Phys.*, 18\(3\), 1495–1506, doi:https://doi.org/10.5194/acp-18-1495-2018, 2018.](#)

Dal Maso, M., Kulmala, M., Riipinen, I., Wagner, R., Hussein, T., Aalto, P. P. and Lehtinen, K. E.: Formation and growth of fresh atmospheric aerosols: eight years of aerosol size distribution data from SMEAR II, Hyytiälä, Finland, *Boreal Environ. Res.*, 10(5), 323, 2005.

Dunne, E. M., Gordon, H., Kürten, A., Almeida, J., Duplissy, J., Williamson, C., Ortega, I. K., Pringle, K. J., Adamov, A., Baltensperger, U., Barmet, P., Benduhn, F., Bianchi, F., Breitenlechner, M., Clarke, A., Curtius, J., Dommen, J., Donahue, N. M., Ehrhart, S., Flagan, R. C., Franchin, A., Guida, R., Hakala, J., Hansel, A., Heinritzi, M., Jokinen, T., Kangasluoma, J., Kirkby, J., Kulmala, M., Kupc, A., Lawler, M. J., Lehtipalo, K., Makhmutov, V., Mann, G., Mathot, S., Merikanto, J., Miettinen, P., Nenes, A., Onnela, A., Rap, A., Reddington, C. L. S., Riccobono, F., Richards, N. A.

D., Rissanen, M. P., Rondo, L., Sarnela, N., Schobesberger, S., Sengupta, K., Simon, M., Sipilä, M., Smith, J. N., Stozkhov, Y., Tomé, A., Tröstl, J., Wagner, P. E., Wimmer, D., Winkler, P. M., Worsnop, D. R. and Carslaw, K. S.: Global atmospheric particle formation from CERN CLOUD measurements, *Science*, 354(6316), 1119–1124, doi:10.1126/science.aaf2649, 2016.

Gordon, H., Kirkby, J., Baltensperger, U., Bianchi, F., Breitenlechner, M., Curtius, J., Dias, A., Dommen, J., Donahue, N. M., Dunne, E. M., Duplissy, J., Ehrhart, S., Flagan, R. C., Frege, C., Fuchs, C., Hansel, A., Hoyle, C. R., Kulmala, M., Kürten, A., Lehtipalo, K., Makhmutov, V., Molteni, U., Rissanen, M. P., Stozkhov, Y., Tröstl, J., Tsagkogeorgas, G., Wagner, R., Williamson, C., Wimmer, D., Winkler, P. M., Yan, C. and Carslaw, K. S.: Causes and importance of new particle formation in the present-day and preindustrial atmospheres, *J. Geophys. Res. Atmospheres*, 122(16), 8739–8760, doi:10.1002/2017JD026844, 2017.

[Größ, J., Hamed, A., Sonntag, A., Spindler, G., Manninen, H. E., Nieminen, T., Kulmala, M., Hörrak, U., Plass-Dülmer, C., Wiedensohler, A. and Birmili, W.: Atmospheric new particle formation at the research station Melpitz, Germany: connection with gaseous precursors and meteorological parameters, *Atmospheric Chem. Phys.*, 18\(3\), 1835–1861, doi:https://doi.org/10.5194/acp-18-1835-2018, 2018.](https://doi.org/10.5194/acp-18-1835-2018)

Hari, P. and Kulmala, M.: Station for measuring ecosystem-atmosphere relations (SMEAR II), *Boreal Environ. Res.*, 10(5), 315–322, 2005.

[Junkermann, W. and Hacker, J. M.: Ultrafine Particles in the Lower Troposphere: Major Sources, Invisible Plumes, and Meteorological Transport Processes, *Bull. Am. Meteorol. Soc.*, 99\(12\), 2587–2602, doi:10.1175/BAMS-D-18-0075.1, 2018.](https://doi.org/10.1175/BAMS-D-18-0075.1)

Junninen, H., Lauri, A., Keronen, P., Aalto, P., Hiltunen, V., Hari, P. and Kulmala, M.: Smart-SMEAR: on-line data exploration and visualization tool for SMEAR stations., *Boreal Environ. Res.*, 14(4), 447–457, 2009.

Keeler, E., Coulter, R., Kyrouac, J. and Holdridge, D.: Balloon-Borne Sounding System (SONDEWNP), *Atmospheric Radiat. Meas. ARM User Facil.*, doi:10.5439/1021460, 2014.

Kerminen, V.-M., Chen, X., Vakkari, V., Petäjä, T., Kulmala, M. and Bianchi, F.: Atmospheric new particle formation and growth: review of field observations, *Environ. Res. Lett.*, 13(10), 103003, doi:10.1088/1748-9326/aadf3c, 2018.

Kulmala, M., Vehkamäki, H., Petäjä, T., Dal Maso, M., Lauri, A., Kerminen, V.-M., Birmili, W. and McMurry, P. H.: Formation and growth rates of ultrafine atmospheric particles: a review of observations, *J. Aerosol Sci.*, 35(2), 143–176, doi:10.1016/j.jaerosci.2003.10.003, 2004.

[Kulmala, M., Petäjä, T., Nieminen, T., Sipilä, M., Manninen, H. E., Lehtipalo, K., Dal Maso, M., Aalto, P. P., Junninen, H., Paasonen, P., Riipinen, I., Lehtinen, K. E. J., Laaksonen, A. and Kerminen, V.-M.: Measurement of the nucleation of atmospheric aerosol particles, *Nat. Protoc.*, 7\(9\), 1651–1667, doi:10.1038/nprot.2012.091, 2012.](https://doi.org/10.1038/nprot.2012.091)

[Laakso, L., Grönholm, T., Kulmala, L., Haapanala, S., Hirsikko, A., Lovejoy, E. R., Kazil, J., Kurten, T., Boy, M., Nilsson, E. D., Sogachev, A., Riipinen, I., Stratmann, F. and Kulmala, M.: Hot-air balloon as a platform for boundary layer profile measurements during particle formation, *Boreal Environ. Res.*, 12\(3\), 279–294, 2007.](https://doi.org/10.1007/s10291-007-0003-0)

Lampilahti, J., Leino, K., Manninen, A., Poutanen, P., Franck, A., Peltola, M., Hietala, P., Beck, L., Dada, L., Quéléver, L., Öhrnberg, R., Zhou, Y., Ekblom, M., Vakkari, V., Zilitinkevich, S., Kerminen, V.-M., Petäjä, T. and Kulmala, M.: Aerosol particle formation in the upper residual layer: dataset, Zenodo, doi:10.5281/zenodo.4063662, 2020.

Leino, K., Lampilahti, J., Poutanen, P., Väänänen, R., Manninen, A., Buenrostro Mazon, S., Dada, L., Franck, A., Wimmer, D., Aalto, P. P., Ahonen, L. R., Enroth, J., Kangasluoma, J., Keronen, P., Korhonen, F., Laakso, H., Matilainen, T., Siivola, E., Manninen, H. E., Lehtipalo, K., Kerminen, V.-M., Petäjä, T. and Kulmala, M.: Vertical profiles of sub-3 nm particles over the boreal forest, *Atmospheric Chem. Phys.*, 19(6), 4127–4138, doi:10.5194/acp-19-4127-2019, 2019.

Manninen, H. E., Petäjä, T., Asmi, E., Riipinen, N., Nieminen, T., Mikkilä, J., Horrak, U., Mirme, A., Mirme, S., Laakso, L., Kerminen, V.-M. and Kulmala, M.: Long-term field measurements of charged and neutral clusters using Neutral cluster and Air Ion Spectrometer (NAIS), *Boreal Environ. Res.*, 14(4), 591–605, 2009.

[Meskhidze, N., Jaimes Correa, J. C., Petters, M. D., Royalty, T. M., Phillips, B. N., Zimmerman, A. and Reed, R.: Possible Wintertime Sources of Fine Particles in an Urban Environment, *J. Geophys. Res. Atmospheres*, 124\(23\), 13055–13070, doi:https://doi.org/10.1029/2019JD031367, 2019.](#)

Mirme, S. and Mirme, A.: The mathematical principles and design of the NAIS – a spectrometer for the measurement of cluster ion and nanometer aerosol size distributions, *Atmospheric Meas. Tech.*, 6(4), 1061–1071, doi:10.5194/amt-6-1061-2013, 2013.

[Nieminen, T., Asmi, A., Dal Maso, M., Aalto, P. P., Keronen, P., Petäjä, T., Kulmala, M. and Kerminen, V.-M.: Trends in atmospheric new-particle formation: 16 years of observations in a boreal-forest environment, *Boreal Environ. Res.*, 19, 191–214, 2014.](#)

Nikandrova, A., Tabakova, K., Manninen, A., Väänänen, R., Petäjä, T., Kulmala, M., Kerminen, V.-M. and O'Connor, E.: Combining airborne in situ and ground-based lidar measurements for attribution of aerosol layers, *Atmospheric Chem. Phys.*, 18(14), 10575–10591, doi:https://doi.org/10.5194/acp-18-10575-2018, 2018.

Nilsson, E. D. and Kulmala, M.: The potential for atmospheric mixing processes to enhance the binary nucleation rate, *J. Geophys. Res. Atmospheres*, 103(D1), 1381–1389, doi:10.1029/97JD02629, 1998.

[Nilsson, E. D., Rannik, Ü., Kulmala, M., Buzorius, G. and O'dowd, C. D.: Effects of continental boundary layer evolution, convection, turbulence and entrainment, on aerosol formation, *Tellus B*, 53\(4\), 441–461, doi:10.1034/j.1600-0889.2001.530409.x, 2001.](#)

O'Connor, E. J., Illingworth, A. J., Brooks, I. M., Westbrook, C. D., Hogan, R. J., Davies, F. and Brooks, B. J.: A Method for Estimating the Turbulent Kinetic Energy Dissipation Rate from a Vertically Pointing Doppler Lidar, and Independent Evaluation from Balloon-Borne In Situ Measurements, *J. Atmospheric Ocean. Technol.*, 27(10), 1652–1664, doi:10.1175/2010JTECHA1455.1, 2010.

[O'Dowd, C. D., Yoon, Y. J., Junkermann, W., Aalto, P., Kulmala, M., Lihavainen, H. and Viisanen, Y.: Airborne measurements of nucleation mode particles II: boreal forest nucleation events, *Atmospheric Chem. Phys.*, 9\(3\), 937–944, doi:10.5194/acp-9-937-2009, 2009.](#)

- Pearson, G., Davies, F. and Collier, C.: An Analysis of the Performance of the UFAM Pulsed Doppler Lidar for Observing the Boundary Layer, *J. Atmospheric Ocean. Technol.*, 26(2), 240–250, doi:10.1175/2008JTECHA1128.1, 2009.
- Petäjä, T., O'Connor, E. J., Moisseev, D., Sinclair, V. A., Manninen, A. J., Väänänen, R., von Lerber, A., Thornton, J. A., Nicoll, K., Petersen, W., Chandrasekar, V., Smith, J. N., Winkler, P. M., Krüger, O., Hakola, H., Timonen, H., Brus, D., Laurila, T., Asmi, E., Riekkola, M.-L., Mona, L., Massoli, P., Engelmann, R., Komppula, M., Wang, J., Kuang, C., Bäck, J., Virtanen, A., Levula, J., Ritsche, M. and Hickmon, N.: BAECC: A Field Campaign to Elucidate the Impact of Biogenic Aerosols on Clouds and Climate, *Bull. Am. Meteorol. Soc.*, 97(10), 1909–1928, doi:10.1175/BAMS-D-14-00199.1, 2016.
- Pierce, J. R. and Adams, P. J.: Uncertainty in global CCN concentrations from uncertain aerosol nucleation and primary emission rates, *Atmospheric Chem. Phys.*, 9(4), 1339–1356, doi:10.5194/acp-9-1339-2009, 2009.
- Platis, A., Altstädter, B., Wehner, B., Wildmann, N., Lampert, A., Hermann, M., Birmili, W. and Bange, J.: An Observational Case Study on the Influence of Atmospheric Boundary-Layer Dynamics on New Particle Formation, *Bound.-Layer Meteorol.*, 158(1), 67–92, doi:10.1007/s10546-015-0084-y, 2015.
- Posner, L. N. and Pandis, S. N.: Sources of ultrafine particles in the Eastern United States, *Atmos. Environ.*, 111, 103–112, doi:10.1016/j.atmosenv.2015.03.033, 2015.
- ~~Qi, X., Ding, A., Nie, W., Chi, X., Huang, X., Xu, Z., Wang, T., Wang, Z., Wang, J., Sun, P., Zhang, Q., Huo, J., Wang, D., Bian, Q., Zhou, L., Zhang, Q., Ning, Z., Fei, D., Xiu, G. and Fu, Q.: Direct measurement of new particle formation based on tethered airship around the top of the planetary boundary layer in eastern China, *Atmos. Environ.*, 209, 92–101, doi:10.1016/j.atmosenv.2019.04.024, 2019.~~
- ~~Quan, J., Liu, Y., Liu, Q., Jia, X., Li, X., Gao, Y., Ding, D., Li, J. and Wang, Z.: Anthropogenic pollution elevates the peak height of new particle formation from planetary boundary layer to lower free troposphere, *Geophys. Res. Lett.*, 44(14), 7537–7543, doi:10.1002/2017GL074553, 2017.~~
- Rose, C., Sellegri, K., Moreno, I., Velarde, F., Ramonet, M., Weinhold, K., Krejci, R., Andrade, M., Wiedensohler, A., Ginot, P. and Laj, P.: CCN production by new particle formation in the free troposphere, *Atmospheric Chem. Phys.*, 17(2), 1529–1541, doi:https://doi.org/10.5194/acp-17-1529-2017, 2017.
- Salma, I., Varga, V. and Németh, Z.: Quantification of an atmospheric nucleation and growth process as a single source of aerosol particles in a city, *Atmospheric Chem. Phys.*, 17(24), 15007–15017, doi:https://doi.org/10.5194/acp-17-15007-2017, 2017.
- Schobesberger, S., Väänänen, R., Leino, K., Virkkula, A., Backman, J., Pohja, T., Siivola, E., Franchin, A., Mikkilä, J., Paramonov, M., Aalto, P. P., Krejci, R., Petäjä, T. and Kulmala, M.: Airborne measurements over the boreal forest of southern Finland during new particle formation events in 2009 and 2010, *Boreal Environ. Res.*, 18(2), 145–164, 2013.
- Siebert, H., Stratmann, F. and Wehner, B.: First observations of increased ultrafine particle number concentrations near the inversion of a continental planetary boundary layer and its relation to ground-based measurements, *Geophys. Res. Lett.*, 31(9), [L09102](#), doi:10.1029/2003GL019086, 2004.

[Stanier, C. O., Khlystov, A. Y. and Pandis, S. N.: Nucleation Events During the Pittsburgh Air Quality Study: Description and Relation to Key Meteorological, Gas Phase, and Aerosol Parameters Special Issue of Aerosol Science and Technology on Findings from the Fine Particulate Matter Supersites Program, *Aerosol Sci. Technol.*, 38\(sup1\), 253–264, doi:10.1080/02786820390229570, 2004.](#)

[Stratmann, F., Siebert, H., Spindler, G., Wehner, B., Althausen, D., Heintzenberg, J., Hellmuth, O., Rinke, R., Schmieder, U., Seidel, C., Tuch, T., Uhrner, U., Wiedensohler, A., Wandinger, U., Wendisch, M., Schell, D. and Stohl, A.: New-particle formation events in a continental boundary layer: first results from the SATURN experiment, *Atmospheric Chem. Phys.*, 3\(5\), 1445–1459, doi:10.5194/acp-3-1445-2003, 2003.](#)

Stull, R. B.: *An Introduction to Boundary Layer Meteorology*, Softcover reprint of the original 1st ed. 1988 edition., Springer, Dordrecht., 1988.

[Takegawa, N., Moteki, N., Oshima, N., Koike, M., Kita, K., Shimizu, A., Sugimoto, N. and Kondo, Y.: Variability of aerosol particle number concentrations observed over the western Pacific in the spring of 2009, *J. Geophys. Res. Atmospheres*, 119\(23\), 13,474-13,488, doi:https://doi.org/10.1002/2014JD022014, 2014.](#)

Väänänen, R., Krejci, R., Manninen, H. E., Manninen, A., Lampilahti, J., Buenrostro Mazon, S., Nieminen, T., Yli-Juuti, T., Kontkanen, J., Asmi, A., Aalto, P. P., Keronen, P., Pohja, T., O'Connor, E., Kerminen, V.-M., Petäjä, T. and Kulmala, M.: Vertical and horizontal variation of aerosol number size distribution in the boreal environment, *Atmospheric Chem. Phys. Discuss.*, Manuscript in review, doi:10.5194/acp-2016-556, 2016.

Vakkari, V., Manninen, A. J., O'Connor, E. J., Schween, J. H., Zyl, P. G. van and Marinou, E.: A novel post-processing algorithm for Halo Doppler lidars, *Atmospheric Meas. Tech.*, 12(2), 839–852, doi:https://doi.org/10.5194/amt-12-839-2019, 2019.

[Venzac, H., Sellegri, K., Laj, P., Villani, P., Bonasoni, P., Marinoni, A., Cristofanelli, P., Calzolari, F., Fuzzi, S., Decesari, S., Facchini, M.-C., Vuillermoz, E. and Verza, G. P.: High frequency new particle formation in the Himalayas, *Proc. Natl. Acad. Sci.*, 105\(41\), 15666–15671, doi:10.1073/pnas.0801355105, 2008.](#)

Wang, J., Krejci, R., Giangrande, S., Kuang, C., Barbosa, H. M. J., Brito, J., Carbone, S., Chi, X., Comstock, J., Ditas, F., Lavric, J., Manninen, H. E., Mei, F., Moran-Zuloaga, D., Pöhlker, C., Pöhlker, M. L., Saturno, J., Schmid, B., Souza, R. A. F., Springston, S. R., Tomlinson, J. M., Toto, T., Walter, D., Wimmer, D., Smith, J. N., Kulmala, M., Machado, L. A. T., Artaxo, P., Andreae, M. O., Petäjä, T. and Martin, S. T.: Amazon boundary layer aerosol concentration sustained by vertical transport during rainfall, *Nature*, 539(7629), 416–419, doi:10.1038/nature19819, 2016.

Wehner, B., Siebert, H., Ansmann, A., Ditas, F., Seifert, P., Stratmann, F., Wiedensohler, A., Apituley, A., Shaw, R. A., Manninen, H. E. and Kulmala, M.: Observations of turbulence-induced new particle formation in the residual layer, *Atmospheric Chem. Phys.*, 10(9), 4319–4330, doi:10.5194/acp-10-4319-2010, 2010.

Williamson, C. J., Kupc, A., Axisa, D., Bilsback, K. R., Bui, T., Campuzano-Jost, P., Dollner, M., Froyd, K. D., Hodshire, A. L., Jimenez, J. L., Kodros, J. K., Luo, G., Murphy, D. M., Nault, B. A., Ray, E. A., Weinzierl, B., Wilson, J. C., Yu, F., Yu, P., Pierce, J. R. and Brock, C. A.: A large source

of cloud condensation nuclei from new particle formation in the tropics, *Nature*, 574(7778), 399–403, doi:10.1038/s41586-019-1638-9, 2019.

Yu, F. and Luo, G.: Simulation of particle size distribution with a global aerosol model: contribution of nucleation to aerosol and CCN number concentrations, *Atmospheric Chem. Phys.*, 9(20), 7691–7710, 2009.

Yu, X., Venecek, M., Kumar, A., Hu, J., Tanrikulu, S., Soon, S.-T., Tran, C., Fairley, D. and Kleeman, M. J.: Regional sources of airborne ultrafine particle number and mass concentrations in California, *Atmospheric Chem. Phys.*, 19(23), 14677–14702, doi:<https://doi.org/10.5194/acp-19-14677-2019>, 2019.

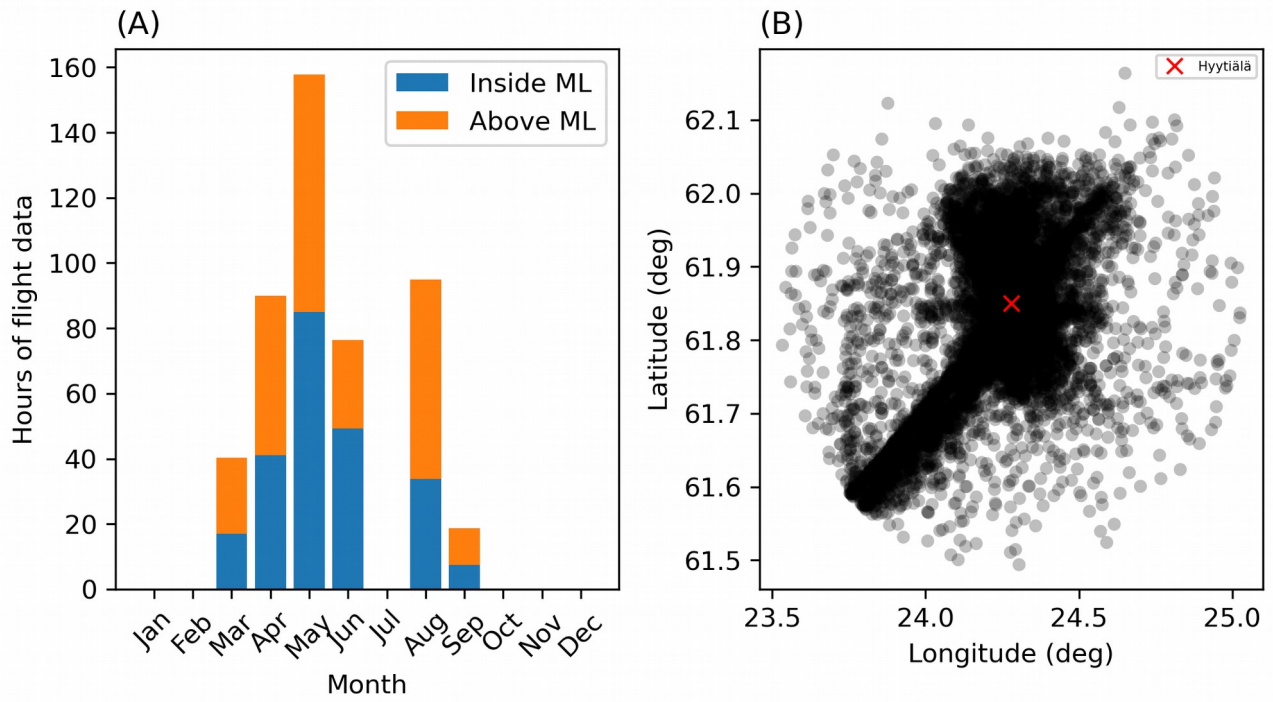
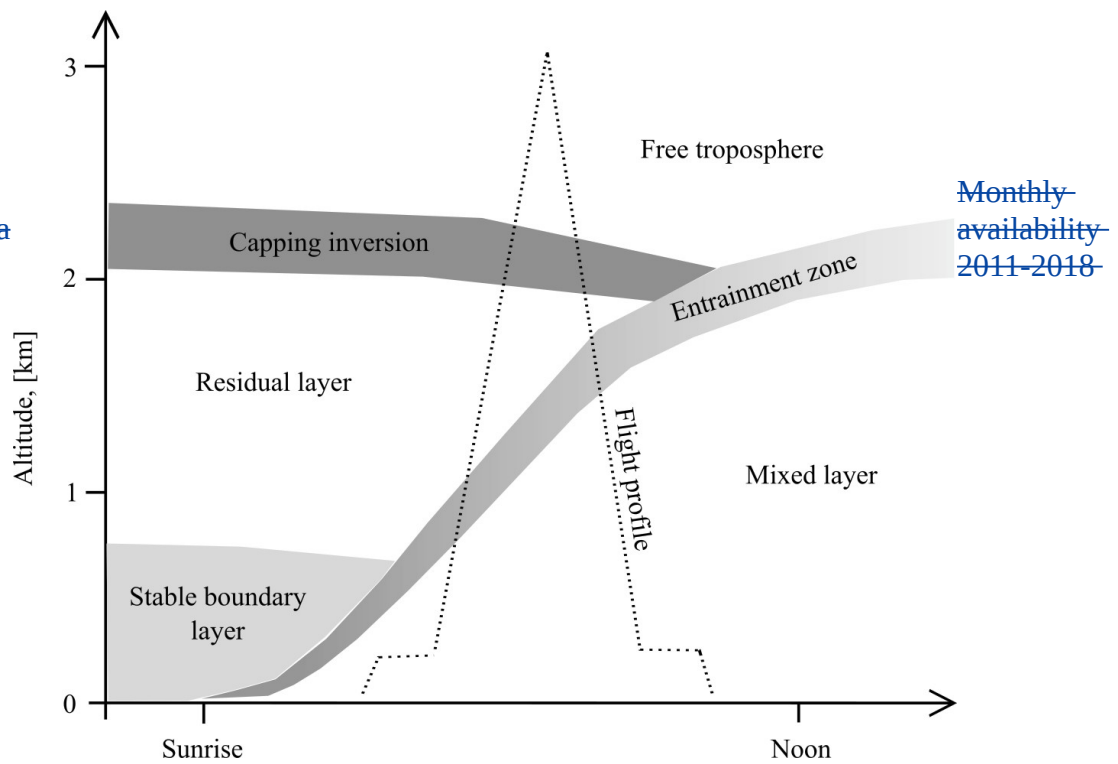


[Figure 1: \(A\) monthly airborne data availability between 2011-2018 divided into measurements above and below the ML, based on the ML height obtained from the ERA5 reanalysis data. \(B\) horizontal distribution of the 2011-2018 airborne measurement data. We chose the data within 40 km radius from Hyytiälä.](#)

Figure 1:
airborne data
between
divided into



measurements above and below the ML, based on the ML height obtained from the ERA5 reanalysis data.

Figure 2: A schematic diagram of an average flight profile in relation to BL evolution.

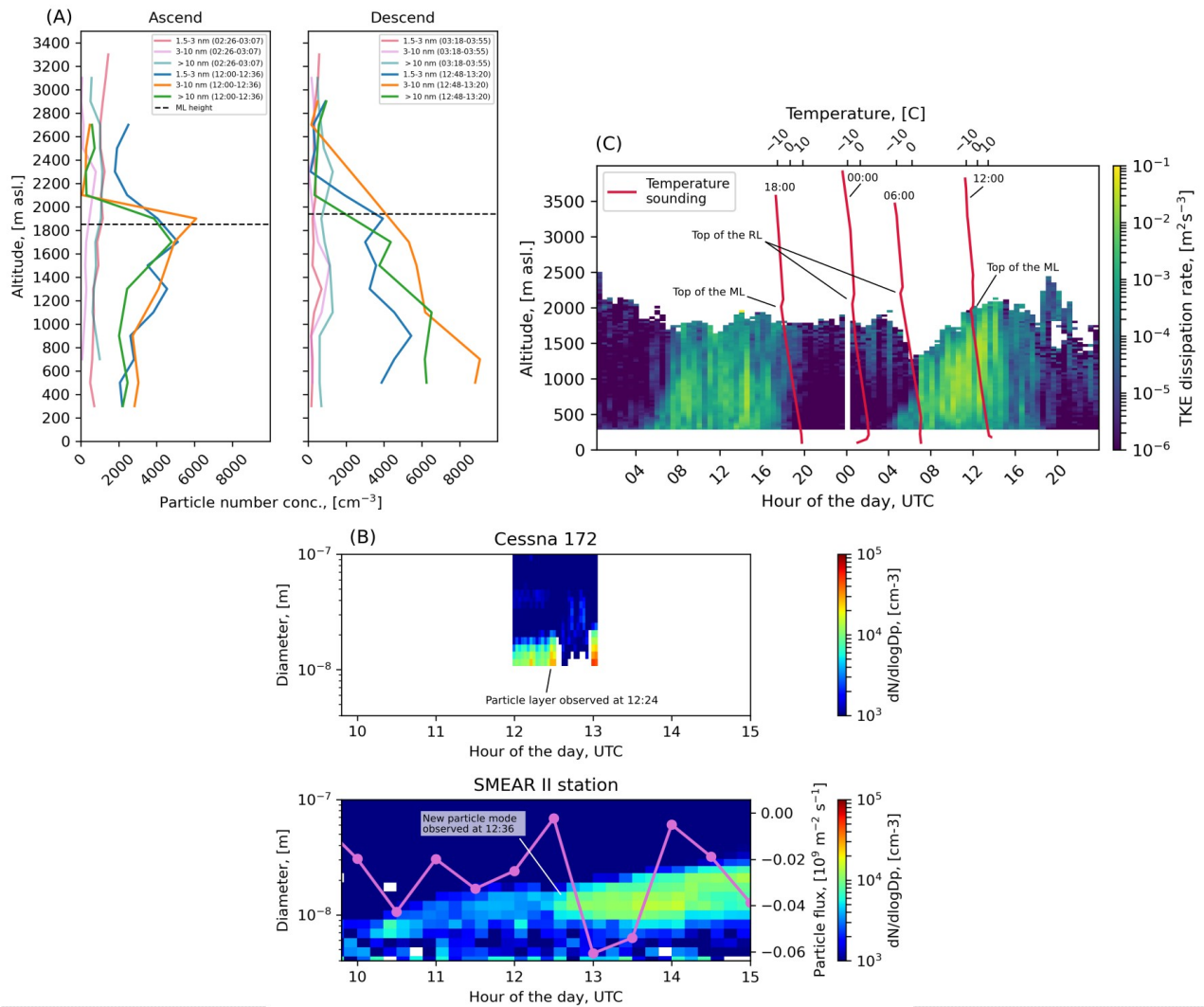


Figure 3: Panel (A) shows vertical profiles of aerosol particle number concentration in three different size ranges (1.5-3 nm, 3-10 nm and >10 nm) on May 2, 2017 (morning flight and afternoon flight). Panel (B) shows the particle number-size distribution from the measurement airplane and the SMEAR II station on May 2, 2017. The vertical flux of >10 nm particles is superimposed. Negative means downward and positive upward particle flux. Panel (C) shows turbulent kinetic energy (TKE) dissipation rate measured by the Doppler lidar in Hyytiälä between May 1-2, 2017. Temperature soundings from Jokioinen are superimposed.

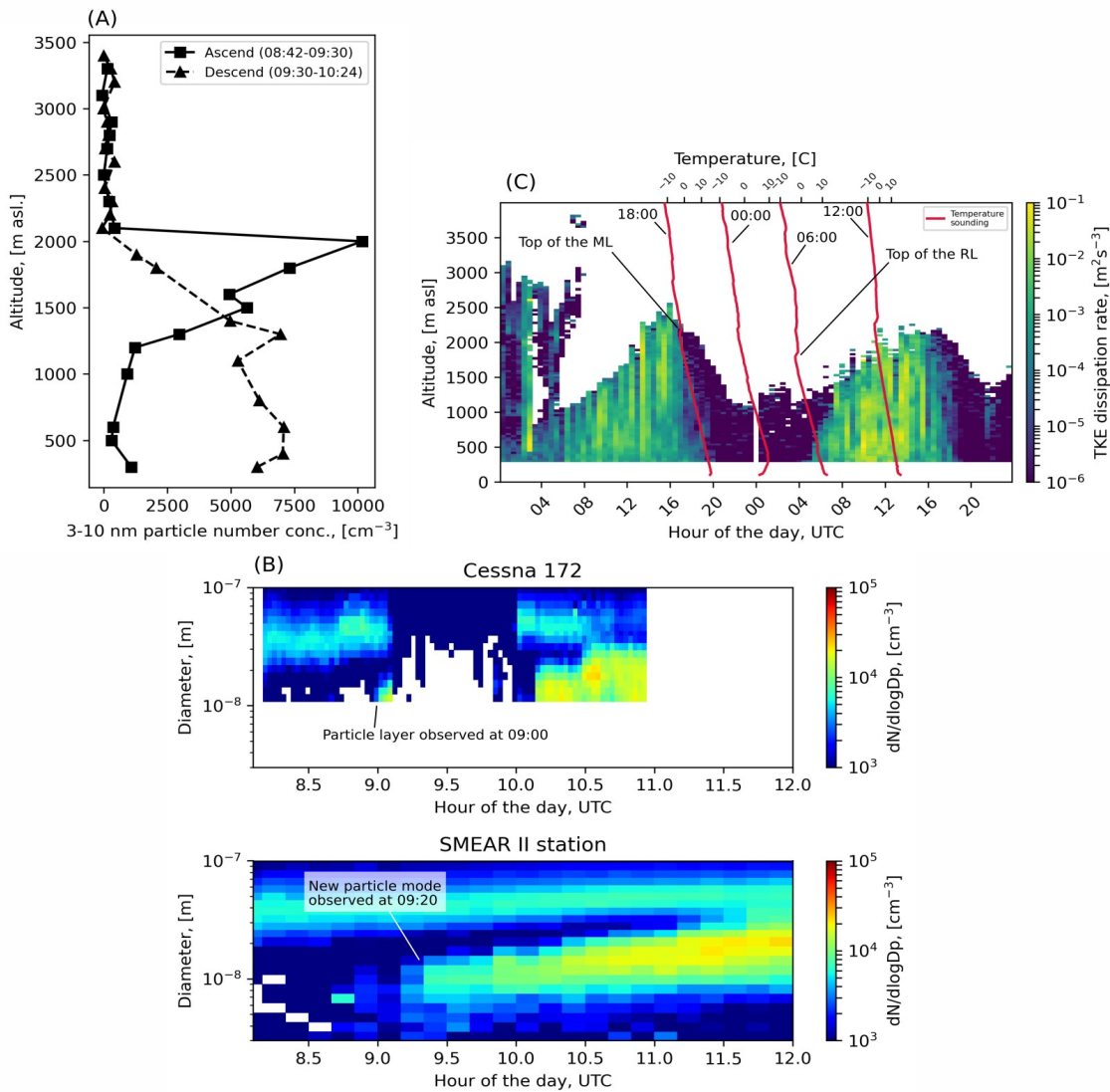


Figure 4: Panel (A) shows vertical profiles of 3-10 nm particle number concentration on May 19, 2017. Panel (B) shows the particle number-size distribution from the measurement airplane and the SMEAR II station on May 19, 2018. Panel (C) shows turbulent kinetic energy (TKE) dissipation rate measured by the Doppler lidar in Hyytiälä between May 18-19, 2018. Temperature soundings from Jokioinen are superimposed.

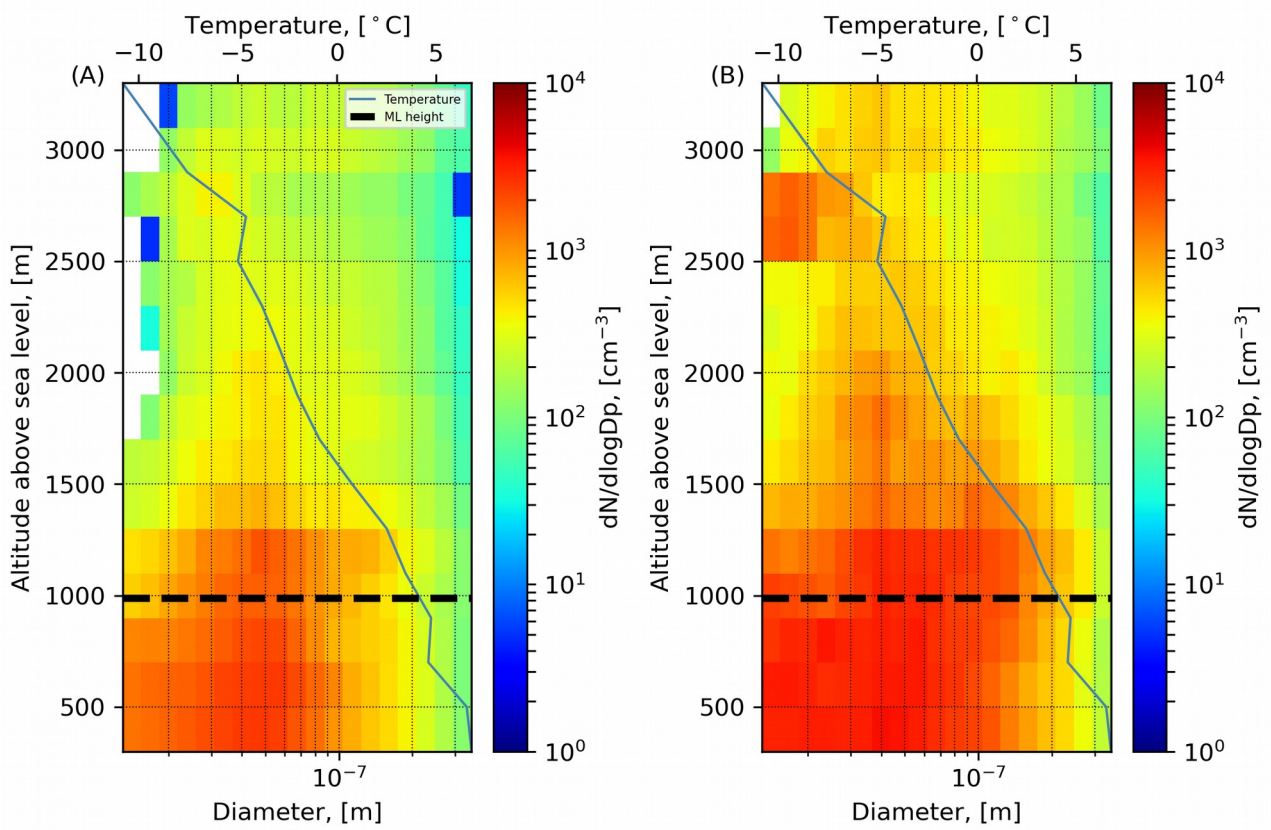


Figure 5: Panel (A) shows the median and panel (B) the 75th percentile vertical profile of particle number-size distribution measured on board the Cessna on NPF event days between 9-12 AM. The number-size distribution was binned into 200 m altitude bins. The data is from the campaigns conducted between 2011-2018. The dashed line is the mean ML height obtained from the ERA5 reanalysis data. The blue line shows the mean temperature profile from measurement flights when the sub-25 nm number concentration in the 2000-3000 m altitude range was above the 75th percentile.

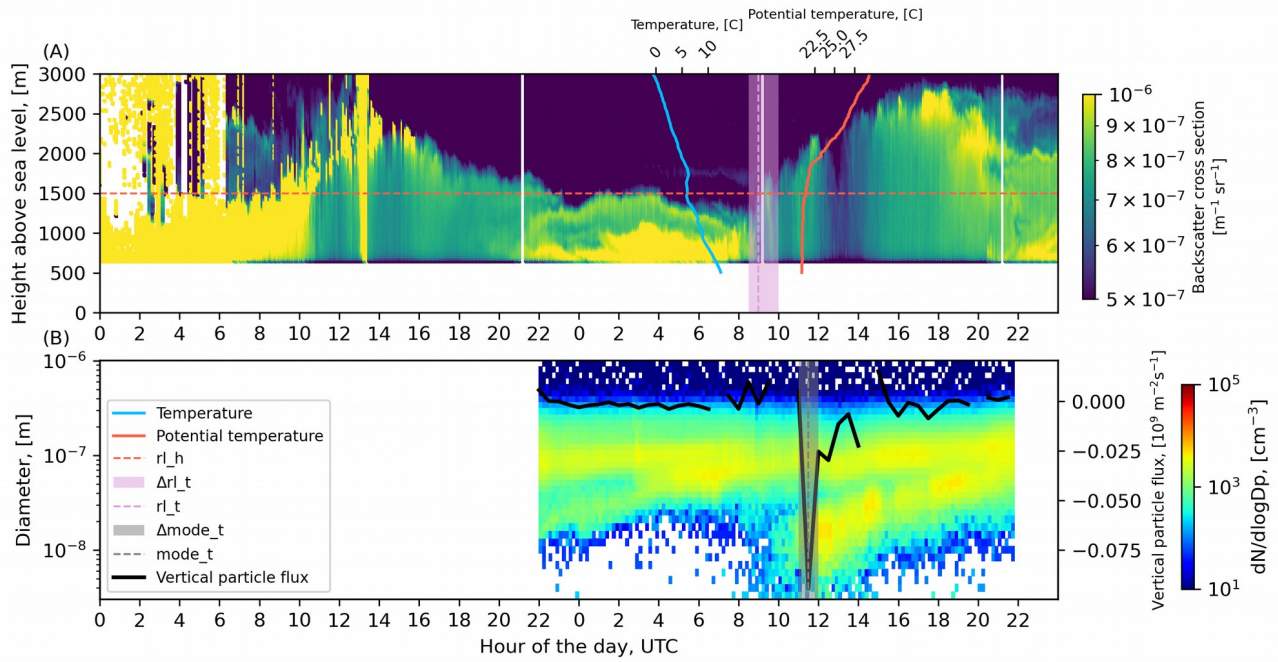
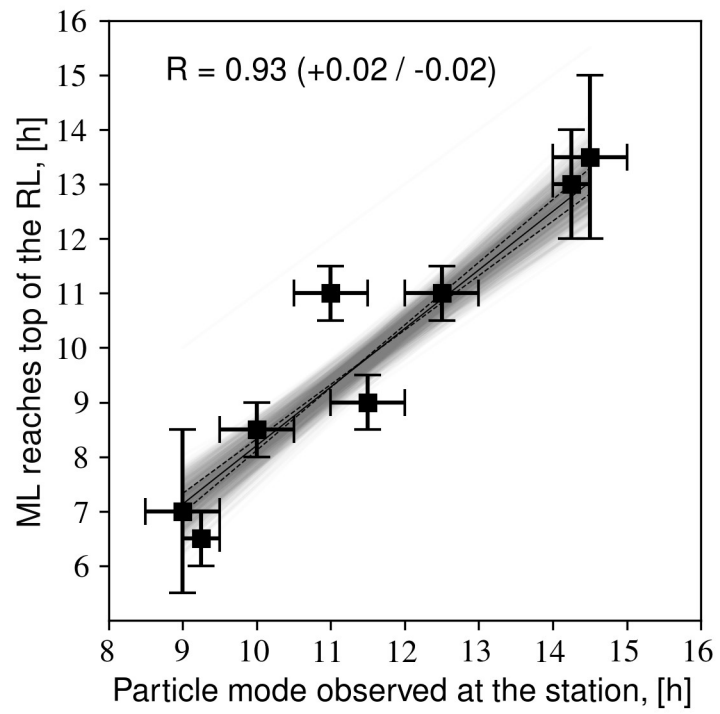
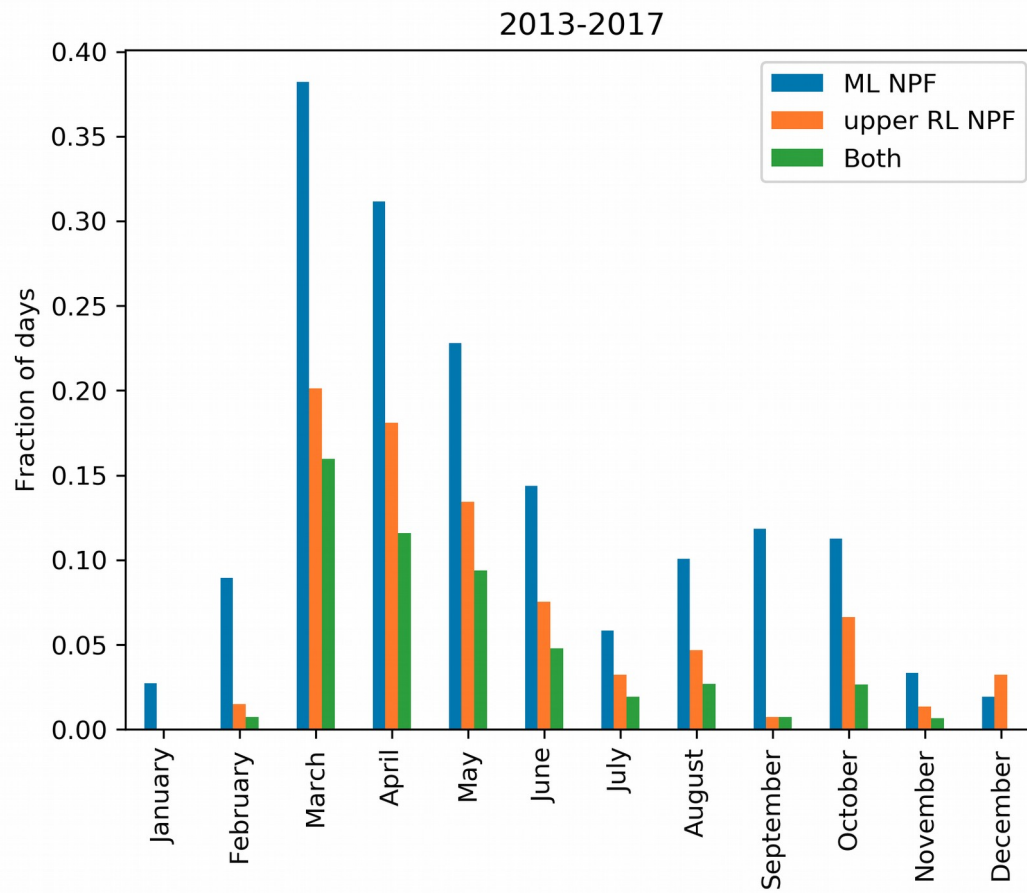


Figure 6: Panel (A) shows the backscatter cross section measured by the HSRL on June 4-5, 2014. The development of the ML is visible from the backscatter cross section signal. Temperature and potential temperature from soundings released in Hyytiälä at 5:20 and 11:20 on June 5, 2014 respectively are superimposed. The horizontal line rl_h refers to the height of the inversion base in the sounding (height of the RL). The rl_t and Δrl_t refer to the time when the ML was estimated to reach the rl_h and the confidence interval for this time, respectively. Panel (B) shows the particle number-size distribution measured at the SMEAR II station, the black line is the vertical particle flux. The $mode_t$ and $\Delta mode_t$ respectively refer to the time and the confidence interval, when a nucleation particle mode that is associated with downward particle flux suddenly appears.



[Figure 7: The correlation between the times that a new particle mode coupled with downward particle flux is observed at the field site and the times that the ML reaches the top of the RL.](#)



[Figure 8: Monthly fractions of NPF within the ML and NPF in the upper RL in Hyttiälä between 2013-2017.](#)

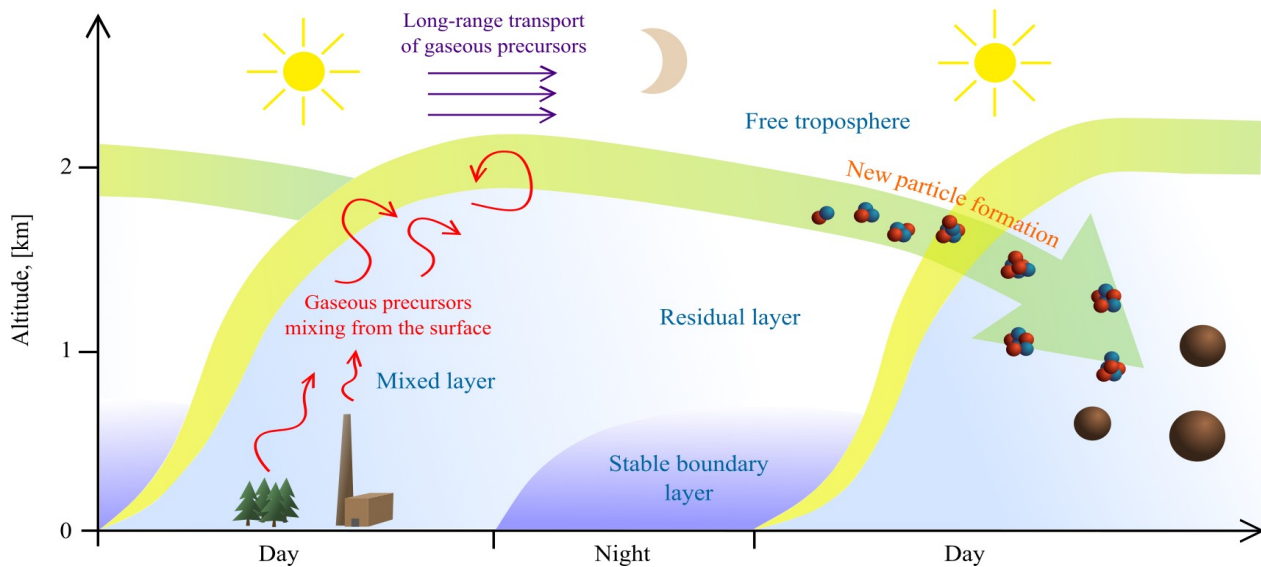


Figure 9: Schematic drawing illustrating the proposed mechanism behind NPF in the upper RL. Gaseous precursors released from biogenic and/or anthropogenic sources are mixed throughout the ML. When the mixing stops during the night the gases are stuck in the RL. Also gaseous precursors may be transported in the FT. In the following morning photochemistry begins and aerosol particles are formed in the interface between the RL and the FT. The freshly formed particles remain in the elevated layer or get mixed into the a new ML if it reaches the height of the upper RL. The aerosol particles continue to grow larger, contributing to the aerosol load in the BL.

Table 1: rl_h = residual layer height during night or early morning (m asl), rl_ht = time when the rl_h was observed (time when the sounding was released, hour of the day, UTC), $mode_t$ = nucleation mode particle mode first appears (hour of the day, UTC), $mode_t1/mode_t2$ = nucleation mode particle mode appearance confidence interval (hour of the day, UTC), rl_t = new mixed layer reaches the top of the residual layer (hour of the day, UTC), rl_t1/rl_t2 = new mixed layer reaches the top of the residual layer confidence interval (hour of the day, UTC), bl_h = observed maximum height of the previous day's boundary layer (m asl.), dp = mean mode diameter for the newly appeared particle mode, when they first appear (nm), gr = growth rate calculated for the newly appeared particle mode ($nm\ h^{-1}$), pf = the value of the negative particle flux peak ($10^9\ m^{-2}\ s^{-1}$).

date	rl_ht	rl_h	mode_t1	mode_t	mode_t2	rl_t1	rl_t	rl_t2	dp	bl_h	pf	gr
20140328	5.3	1100	8.5	9	9.5	5.5	7	8	20	1300	-0.25	2.28
20140331	7.6	2400	14	14.5	15	12	13.5	14	10	2200	-0.06	2.1
20140404	8.5	2200	10.5	11	11.5	10.5	11	11.5	8	2800	-0.04	1.39
20140409	5.5	1500	9	9.25	9.5	6	6.5	7	8	1800	-0.13	1.18
20140415	5.3	1600	14.5	14.25	15	12	13	14	11	1700	-0.18	1.94
20140422	0.0	1800	12	12.5	13	10.5	11	11.5	17	1900	-0.17	1.0
20140518	0.0	1500	9.5	10	10.5	8	8.5	9	13	1900	-0.11	2.91
20140705	5.3	1500	11	11.5	12	8.5	9	10	12	1700	-0.1	4.83

564

Figure 2: A schematic diagram of an average flight profile in relation to boundary layer evolution.

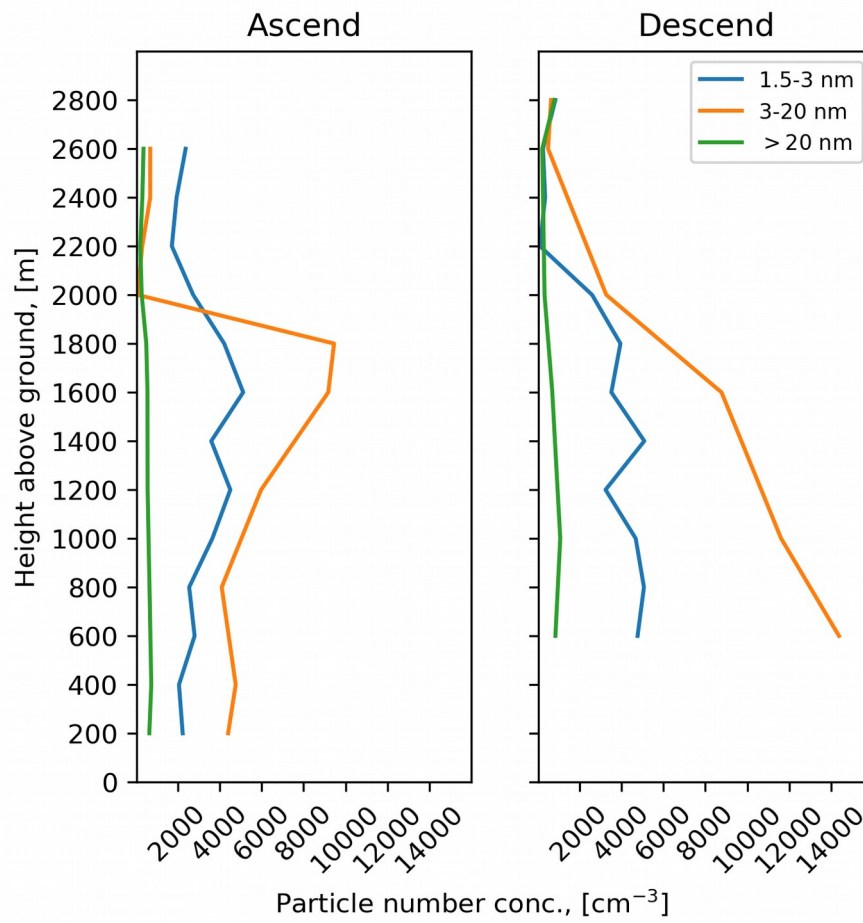


Figure 3: Vertical profiles of aerosol particle number concentration in three different size ranges (1.5-3 nm, 3-20 nm and >20 nm). The measurement profile was done on May 2, 2017 between 09:30 and 12:00 UTC.

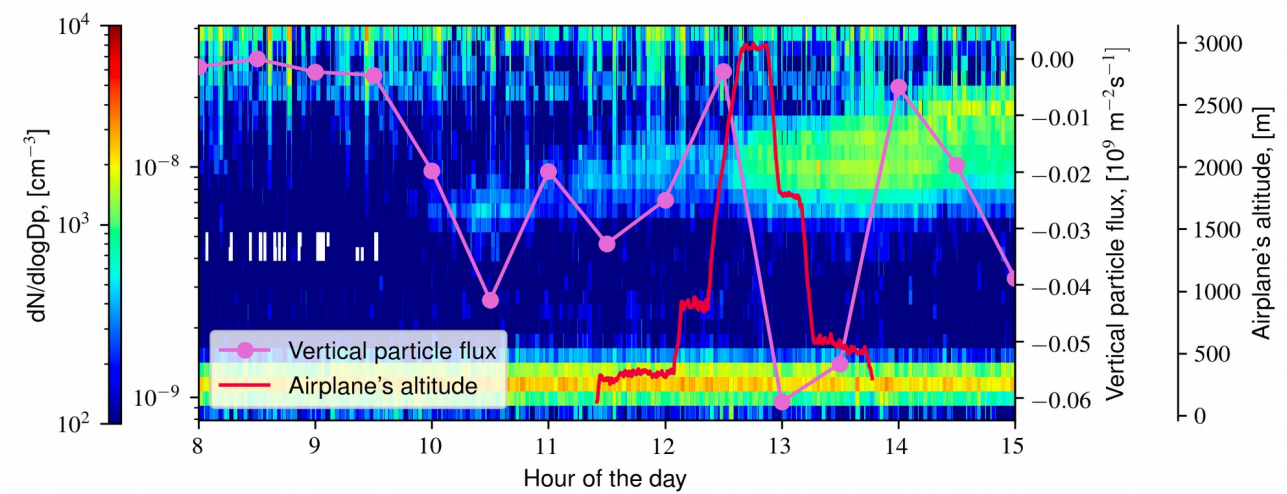


Figure 4: Positive ion number-size distribution measured at the SMEAR II station on May 2, 2017. The vertical flux of >10 nm particles and the airplane's altitude profile are superimposed. Negative means downward and positive upward particle flux.

567
568
569
570
571
572
573
574
575
576
577
578
579
580
581
582
583
584
585
586
587
588

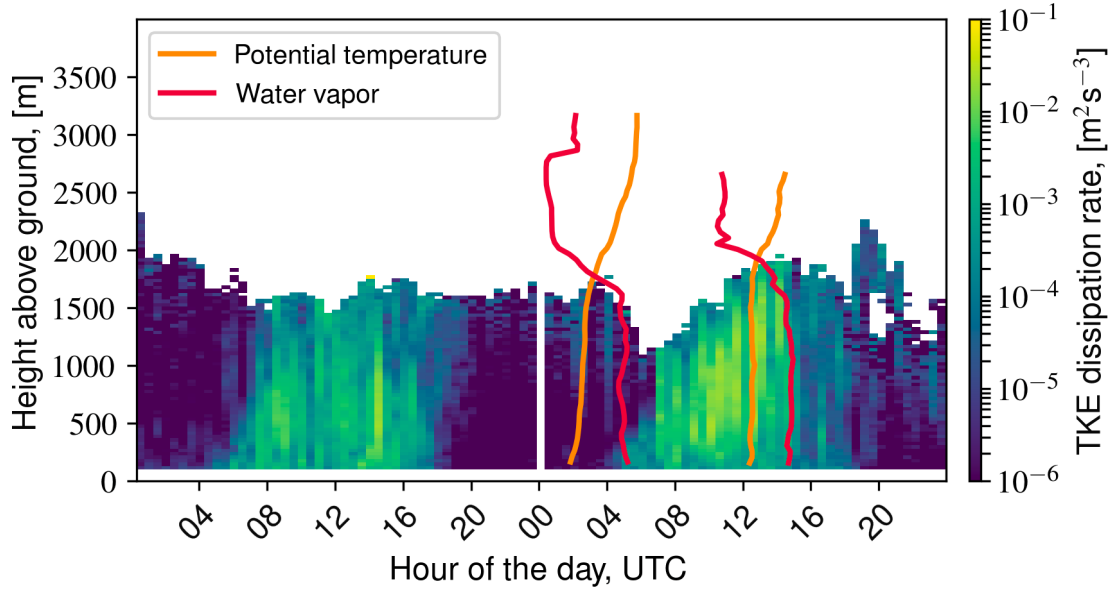


Figure 5: Turbulent kinetic energy (TKE) dissipation rate measured by the Doppler lidar in Hyytiälä between May 1-2, 2017. In addition the vertical profiles of potential temperature and water vapor concentration are shown from both the night and the afternoon Cessna flights on May 2, 2017.

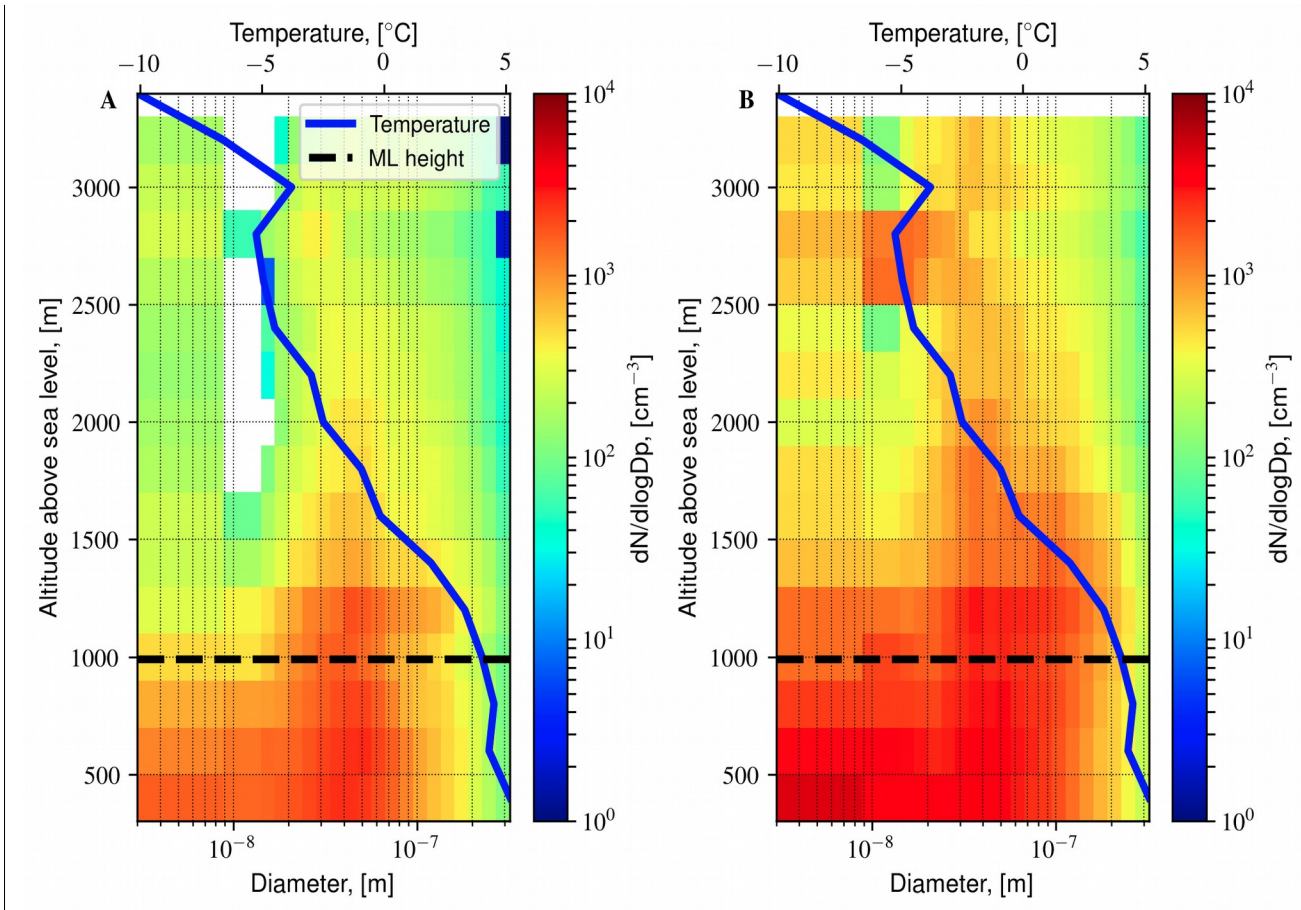


Figure 6: Panel A shows the median and panel B the 75th percentile vertical profile of particle number-size distribution measured on board the Cessna on NPF event days between 9-12 AM. The number-size distribution was binned into 200 m altitude bins. The data is from the campaigns conducted between 2011 and 2018. It includes only the data that was measured within 40 km radius from Hyytiälä. The dashed line is the mean ML height obtained from the ERA5 reanalysis data. The blue line is the mean temperature profile measured on board the airplane.

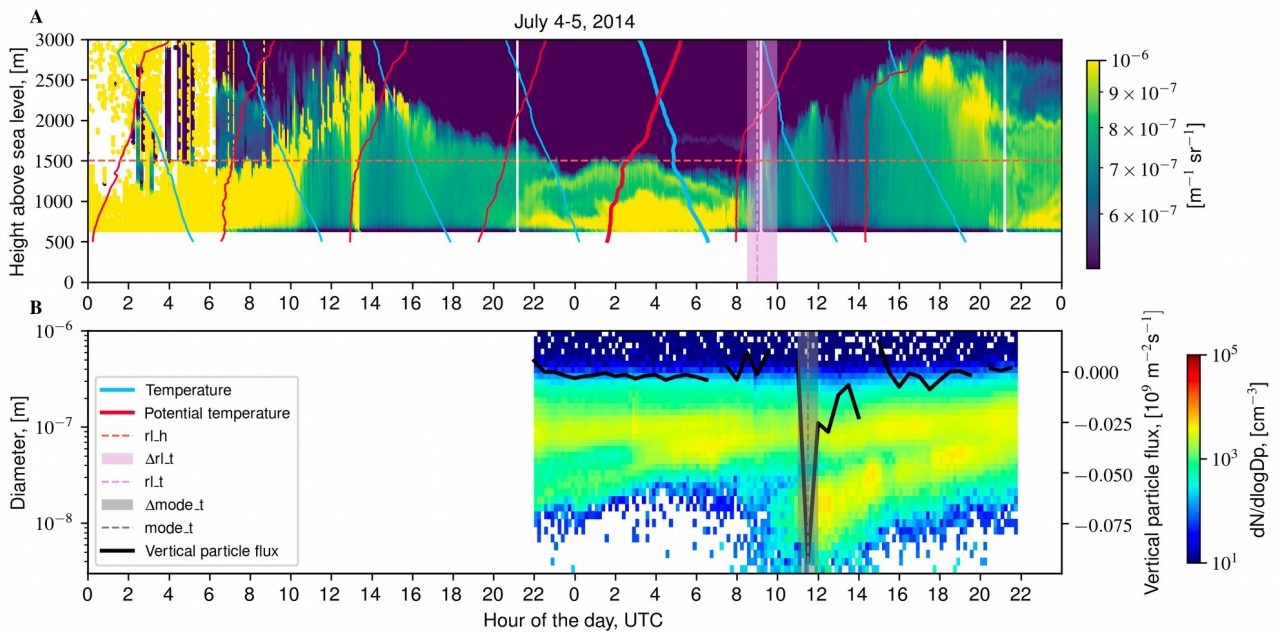


Figure 7: Panel A shows the backscatter cross section measured by the HSRL. The development of the ML is visible from the backscatter cross section signal. Temperature and potential temperature profiles from the 4-hourly balloon soundings are superimposed. The horizontal line rl_h refers to the height of the inversion base observed during the early morning of July 5th. The bold temperature and potential temperature profiles mark the sounding from which rl_h was determined. The rl_t and Δrl_t refer to the time when the ML was estimated to reach the rl_h and the confidence interval for this time respectively. Panel B shows the particle number-size distribution measured at the SMEAR-II station, the black line is the vertical particle flux. The $mode_t$ and $\Delta mode_t$ respectively refer to the time and the confidence interval, when a nucleation particle mode that is associated with downward particle flux suddenly appears.

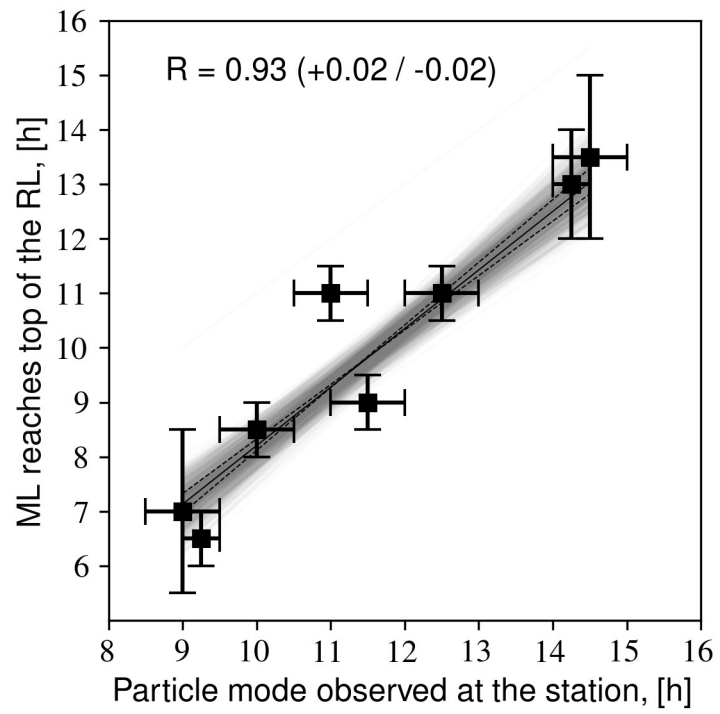


Figure 8: The correlation between the times that a new particle mode coupled with downward particle flux is observed at the field site and the times that the ML reaches the top of the RL.

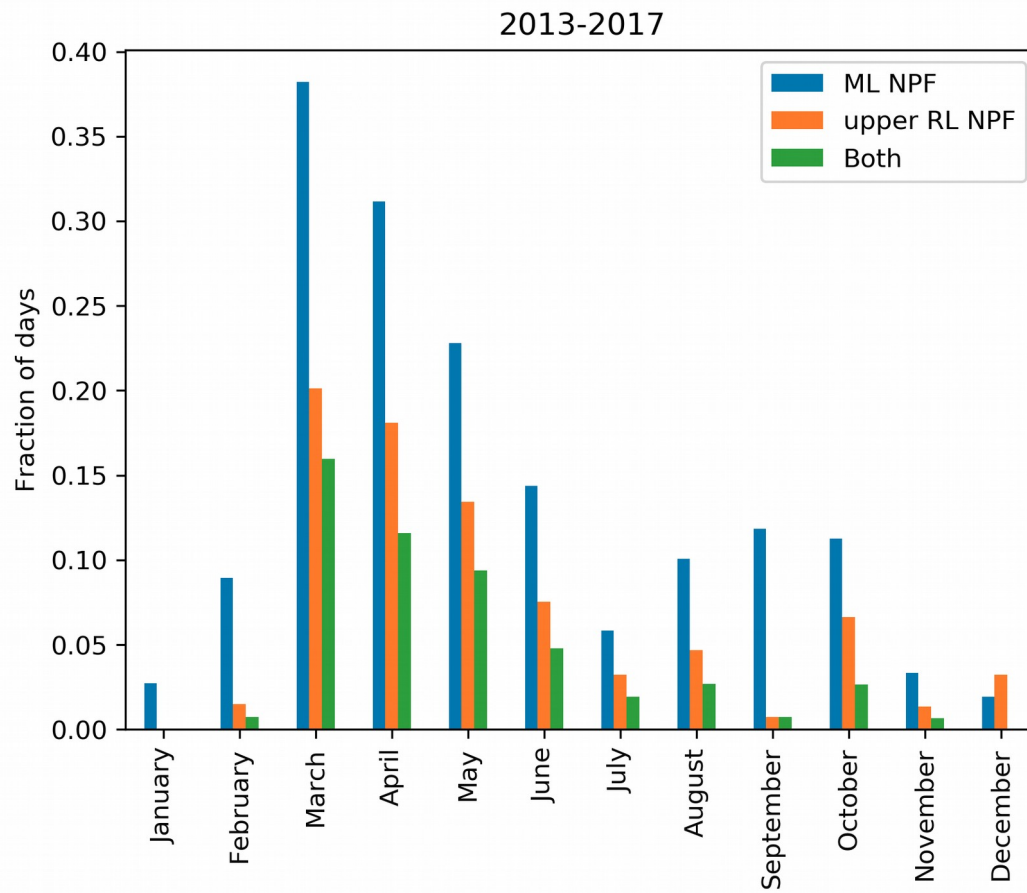


Figure 9: Monthly fractions of NPF within the ML and NPF in the upper RL in Hyttiälä between 2013-2017.

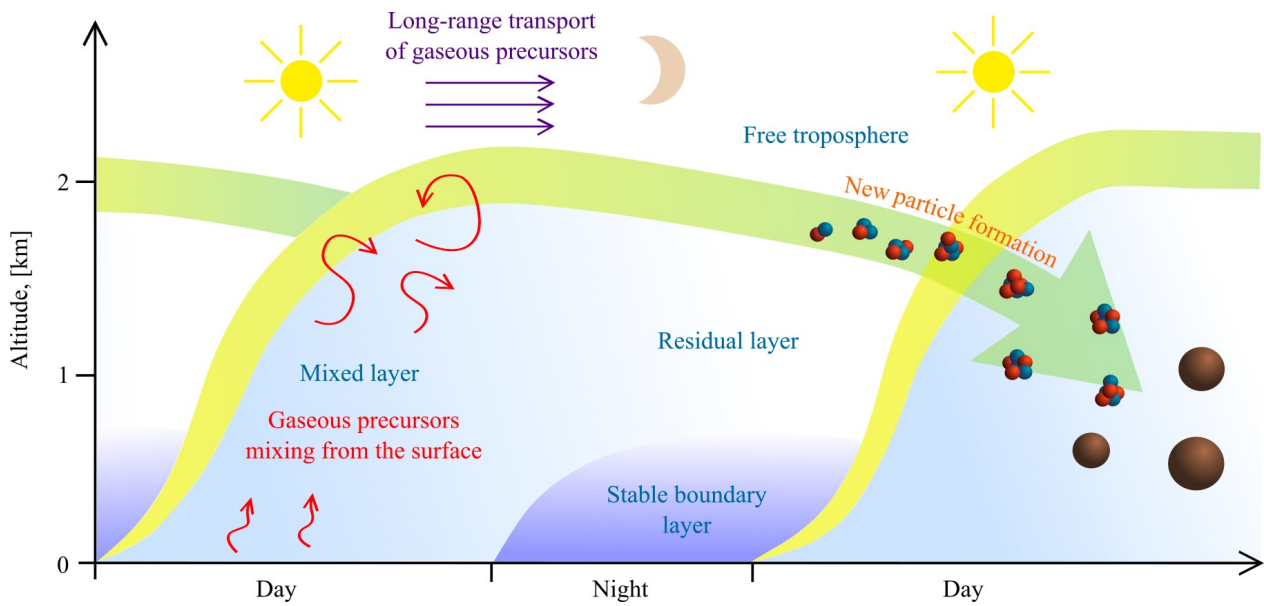


Figure 10: Schematic drawing illustrating the proposed mechanism behind NPF in the upper RL. Gaseous precursors released from the surface are mixed throughout the ML. When the mixing stops during the night the gases are stuck in the RL. Also gaseous precursors may be transported in the FT. In the following morning photochemistry and the thermodynamically favorable conditions in the upper RL initiate NPF. The freshly formed particles remain in the elevated layer or get mixed into the a new ML if it reaches the height of the upper RL. The aerosol particles continue to grow larger, contributing to the aerosol load in the BL.